NTNU

Norwegian University of
Science and Technology

Ground station considerations for the AMOS satellite programme

Øyvind Karlsen

Master of Science in Electronics
Submission date: July 2017
Supervisor: Torbjørn Ekman, IES

Norwegian University of Science and Technology
Department of Electronic Systems

NTNU – Trondheim
Norwegian University of
Science and Technology

Ground station considerations for the AMOS satellite programme

Øyvind Karlsen

July 8, 2017

Problem Description

NTNU has established a new research programme within the CAMOS and AMOS umbrellas. This program focuses on rapidly launching Small Satellites (SmallSats) for maritime applictions. The task is to investigate and specify requirements and methodologies for establishing ground stations to support these rapid satellite launches with coverage in the VHF/UHF/SHF bands.

The thesis should include:

- A study of ground station networks.

- Finalisation and verification of the VHF/UHF ground station for NTNU Test Satellite (NUTS).

- A study of available system subcomponents for GHz range satellite ground stations.

- A proposal for a wideband ground station to support future NTNU satellites.

Abstract

NTNU centre for Autonomous Maritime Operations and Systems (AMOS) is expanding with a satellite programme (AMOS-Sat). These satellites will operate with frequencies ranging from VHF to low SHF. To support these future satellites, NTNU will need more resources in the ground station segment. To get experience with research, development and maintenance of ground stations, these should be built, tested and used to conduct research.

For easy access to and distribution of satellite data, a network service must be considered. An alternative to high cost commercial solutions is an open ground station network. A survey of such platforms is conducted. One of the platforms, SatNOGS, is further explored by setting up a VHF/UHF network node. This network node has tracked and recorded over 200 satellite passes during the spring of 2017.

The build and verification of the VHF/UHF ground station is presented. The results are used to form a link budget. It shows that the ground station can support orbits up to 400 km for VHF and up to 500 km for UHF in 99% of all fading cases. The results from SatNOGS show that the station can support much higher orbits but may become scintillation limited.

Finally, a novel idea for a low SHF ground station to support the AMOS-Sat endeavour is presented. The ground station is based on an adaptive polarisation SDR platform, and supports up- and downlink over 1 GHz to 6 GHz.

The ground station for VHF/UHF and future expansion to the GHz range gives NTNU the needed experience in ground station operation. This, together with the potential for an open global network that SatNOGS provides, gives AMOS-Sat a low-cost alternative to commercial ground station services.

Sammendrag

NTNUs senter for Autonome Maritime Operasjoner og Systemer (AMOS) utvider nå med et satellitt-program kalt AMOS-Sat. Disse vil operere i frekvensområdet mellom VHF og lav SHF. For å støtte disse fremtidige satellittene trenger NTNU mer kunnskap og utstyr knyttet til bakkestasjons-segmentet. For å få erfaring med forskning, utvikling og vedlikehold av bakkestasjoner, må disse bli bygd, testet og brukt til forskning.

For enkel tilgang til og for fordeling av satelittdata må en nettverkstjeneste vurderes. Et alternativ til dyre kommersielle løsninger er et åpent bakkestasjonsnettverk. En undersøkelse av slike nettverk er gjennomført. Ett av disse nettverkene, SatNOGS, er videre undersøkt ved å sette opp en VHF/UHF nettverksnode. Denne nettverksnoden har fulgt og tatt ned data fra over 200 satellittpass i løpet av våren 2017.

Konstruksjon og verifikasjon av VHF/UHF bakkestasjonen er presentert. Resultatene er brukt til å utarbeide et linkbudsjett. Dette visert at bakkestasjonen kan støtte satellittbaner opp til 400 km for VHF og opp til 500 km for UHF i 99% av alle fading-tilfeller. Resultaene fra SatNOGS viser at bakkestasjonen kan støtte høyere baner, men kan bli begrenset av sterk fading fra scintillasjon.

Til slutt presenteres en idé for en lav SHF bakkestasjon for å støtte AMOS satellittene. Bakkestasjonen er basert på en adaptiv-polarisasjons SDR plattform, og støtter opp- og nedlink over frekrensområdet fra 1 GHz til 6 GHz.

Bakkestasjonen for VHF/UHF og fremtidig utvidning til frekvenser i GHz området gir NTNU den erfaringen som trengs med bakkestasjonsdrift. Dette, sammen med potensialet for et åpent globalt bakkestasjonsnettverk gjennom SatNOGS, gir AMOS-Sat et billigere alternativ til kommersielle bakkestasjonstjenester

Contents

1. Introduction and background

Research is ongoing at Norwegian University of Science and Technology (NTNU) to allow for better utilisation of the large Norwegian coastline. One of the driving research projects is NTNUs centre for Autonomous Marine Operations and Systems (AMOS).

In 2017 the AMOS Satellite (AMOS-Sat) programme is started. AMOS-Sat is a Small Satellite (SmallSat) programme that will support and enable more sophisticated surveillance, automation and operations in the arctic ocean space. [1]

For polar communications, Geostationary Earth Orbit (GEO) satellites do not provide the needed coverage. Instead Low Earth Orbit (LEO) satellites in polar orbits are used [2]. Polar orbit satellites have become of great importance for modern communication systems in the northern hemisphere. Two such systems are the automatic identification system (AIS) [3] and the upcoming Very High Frequency (VHF) data exchange system (VDES) [4].

Launching satellites to LEO is significantly cheaper than launching to GEO, but the ground station may become more complex as tracking must be applied for high datarate applications. Current Telemetry, Tracking and Command (TT&C) efforts for non-stationary satellite orbits at NTNU consist of an incomplete Cube Satellite (CubeSat) ground station in the VHF/ Ultra High Frequency (UHF) amateur radio bands for NTNU Test Satellite (NUTS). This station is referred to as the Gløshaugen ground station in this thesis.

One of the goals of the AMOS-Sat project is yearly back-to-back launches of several SmallSats. For this to be realisable a reliable ground station that can be rapidly reconfigured to support various missions is needed. If AMOS-Sat is to be successful, NTNU must become more active in the ground segment of satellite operations. This thesis investigates options for doing so.

For non-commercial satellite missions (e.g. CubeSats), global ground station coverage is still a challenge. Usually only one headquarter is available and more stations in the ground segment imply either complex arrangements with other groups or high rental costs. While there is no satellite to serve yet, a NTNU ground station can assist other research institutions and interested third parties with their missions. One way to do this is to set up an open ground station network node. An open ground station network is a user contributed network where data from satellites

are shared between different ground stations and satellite operators, possibly also interested third parties. By participating in a network, we get access to the other ground stations in the network. This can be useful for future NTNU research.

The idea of open networked ground stations is not new. Global Educational Network for Satellite Operations (GENSO) [5] was one of the early drivers already in 2006. As of 2017, there are more options such as Satellite networked open ground station (SatNOGS) [6], Distributed Ground Station Network (DGSN) [7], ThumbNet [8] as well as a relaunch of GENSO in a 2.0 version. To get a better idea of what to expect from the different services, and which one is most suitable for NTNU, a survey must be conducted.

Experience with ground station operation will be crucial when designing the next generation of ground terminals that will serve AMOS-Sat. To get this experience, the NUTS ground station must be put into service. The ground station should build on Software Defined Radio (SDR) to be rapidly deployable and re-configurable for different applications. SDR based ground stations are well established, Leffke [9] and Dascal [10] present receive only solutions for tracking VHF/UHF ground stations on SDR platforms. Bosco [11] describes a receive and transmit capable SDR solution for the UHF amateur radio band.

Some of the potential sensor payloads for the AMOS-Sat project are a hyper-spectral camera and a synthetic aperture radar [1]. These applications require high amounts of data to be transferred over the satellite downlink. These data rates are not realisable over the previously discussed amateur radio VHF/UHF links, as the allowed transmission bandwidth is too low [12]. To get the required data rate, the ground station must move to frequencies in the high UHF and low Super High Frequency (SHF) band [2]. While there are many commercial ground station services available for these frequencies, development will likely be cheaper using a dedicated on-site ground station. Being able to do initial tests, debugging and testing without paying for network time is valuable. In order to do this, research into viable solutions for network services must be conducted.

The local student amateur radio club (ARK) is also interested in expanding coverage into the amateur radio bands between 1 GHz and 10 GHz. This provides a unique opportunity to test some of the components for a NTNU ground station before committing resources.

The remainder of the report has the following structure. Chapter 2 outlines various networked ground station services. In chapter 3 the build and verification of a VHF/UHF CubeSat ground station is detailed. A feasibility study for a future adaptive multipurpose wideband ground station is conducted in chapter 4. The report is concluded by Chapter 5, which also holds notes for future work.

2. Networked ground stations

For research endeavours with limited budgets, global ground station coverage is a challenge. Extended coverage is needed to gather scientific data that the mission requires. This coverage comes at a price, either through commercial rental or time consuming arrangements with other institutions.

University ground stations are often unused, even when they are actively participating in satellite campaigns. This is the nature of non-stationary orbits, as the satellite only is visible over the horizon part of the time [2].

During downtime the ground station can contribute to other satellite missions, by tracking their satellite if the satellite is visible. To make this process simple a satellite network service is utilised. The role of the network service is to act as an information broker between ground stations and third parties.

To illustrate why networked ground stations are important the downlink availability of a fictional polar orbiting satellite, DemoSat, is simulated over six days using System Toolkit [13]. The results are seen in figure 2.1. The figures illustrate how adding additional ground stations increases the time a satellite can be supported.

An open networked ground station service is interesting for both NTNU and AMOS-Sat. This network can enable science that would previously be very expensive to conduct, for example radio channel measurements on a world-wide level. For AMOS-Sat the additional ground support will be helpful during launch, debugging and development. A network service that also incorporates examples or solutions for automated tracking and recording is desirable. Time to research can be reduced if the operator can use a readily available solution rather than writing it from scratch.

In this chapter different networked ground station solutions are surveyed, and the Gløshaugen site station is set up as a SatNOGS node.

2.1. Platform survey

In order to chose one or several network services to participate in, a small survey of their functionality is presented. Note that this assessment is made during the

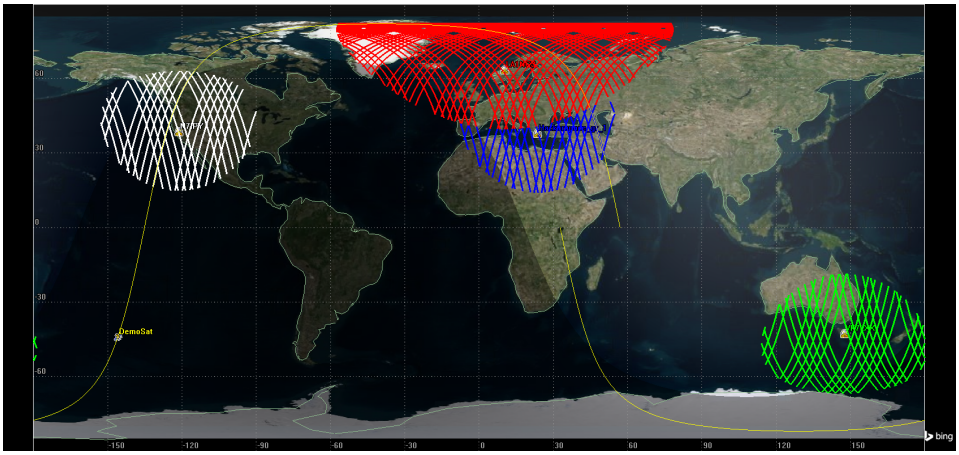

(a) Supportable DemoSat passes. White, red, blue and green traces show viable passes for each ground station.

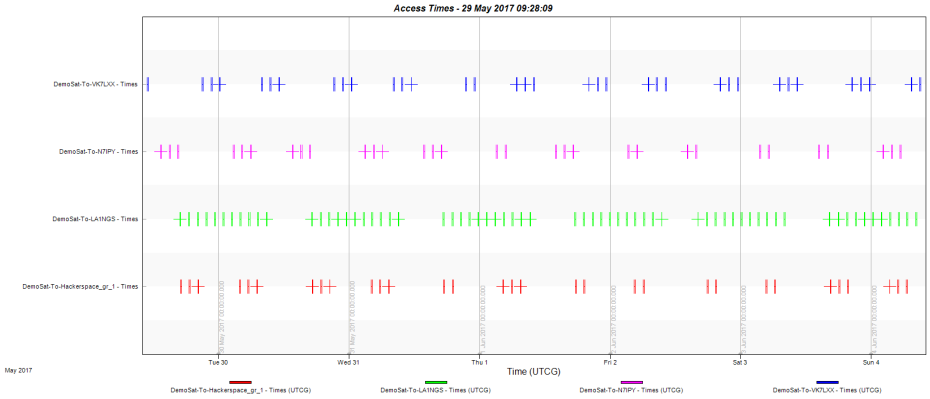

(b) Access times to DemoSat for different ground stations.

Figure 2.1.: Simulated downlink availability over six days for a fictional satellite.

spring of 2017, and any updates to the software after this will not be reflected.

2.1.1. SatNOGS

SatNOGS [6] is an open source initiative developed by the Libre Space Foundation and volunteers. In a wide sense, SatNOGS consists of four components; the network, a satellite database, the client and hardware.

The network [14] is a web service for scheduling satellite observations, accessing past observations and moderating the ground station. There is also a development network[15] where new stations are created and tested before being moved to the production network.

To coordinate satellite state and transponders, SatNOGS provides a database [16]. This database is user-contributed and has an application programming interface (API). The transponder database makes it easier to coordinate with a large range of satellites.

Tracking, recording and data processing is performed by the client [17]. The tracker uses Two Line Element sets (TLEs) to calculate an estimate for the satellite position. Rotctl from hamlib [18] is used to steer the antenna. Satellite data is demodulated using gnuradio [19] modules (GR-SatNOGS [20]) to baseband and then distributed to SatNOGS network as a .ogg audio file. A waterfall image of the audio file is also produced, this way a user can quickly assess if an observation contains data. In the future the client may also perform control and command, as it has done for the UpSat mission [21].

Open source hardware makes SatNOGS an economic solution for ground station adopters. Among the hardware are different antennas [22], a rotor [23] and a controller for the rotor [24].

2.1.2. GENSO 2.0

One of the early drivers in open networked ground station design was the GENSO project [5]. The system was very specific as to which hardware [25] could be used, and how the station had to be integrated. Together with a large codebase and poor outreach this made the system hard to adopt.

GENSO is being relaunched in a 2.0 version, with an alpha/beta stage some time in late 2017. The author attended a meeting with European Space Operations Centre (ESOC), which is responsible for the relaunch. Information presented here is based on meeting notes, and is highly subject to change.

GENSO 2.0 is based on the idea of sharing resources. The core software is a database of available ground stations and storage of data received from satellites. The software is presented as a matchmaking website which matches ground station operators and satellite operators. By providing data to other ground station or satellite operators, the operator is allowed to schedule and gather data from other missions. At this point the web-service is closed source.

2.1.3. Distributed Ground Station Network (DGSN)

DGSN [7] is an idea for a satellite multilateration network. By comparing time of arrival at several receivers with known positions it is possible to accurately pinpoint the location of different objects. When a satellite passes the nodes of the network an estimate of orbital parameters may be derived. The system is not more accurate than radar tracking, but it will have a higher update rate. This makes TLE ageing a smaller issue.

A system like this would be particularly useful in the first days after a satellite has been launched, when TLEs are not yet available.

The software is available open-source on GitHub [26]. The software is at a prototype stage, hence it is unstructured.

2.1.4. Thumbnet

Thumbsat [8] is marketed as an affordable educational platform and targets schools worldwide. The concept is to launch a small satellite where the user only provides a small payload of max 25 grams. Thumbsat provides all other systems, and part of this is the ground station network Thumbnet.

Thumbsat has yet to launch any satellites, but the ground station network already has 250 stations. Based on a low-cost SDR and homemade antennas, the station allows the user to explore the RF spectrum in manual mode. The networked service, also called automatic mode, is limited to thumbsat missions. The software is provided closed-source.

2.2. Platform choice and implementation

The most promising service for a NTNU ground station is SatNOGS. It is similar in many aspects to the other services, but has some features that makes it suitable. It has been used for TT&C for the UpSat [21] mission. The codebase is well defined

and modular [6]. The system supports many SDRs and rotors. Most importantly, it is compatible with the equipment that is already available at the Gløshaugen ground station.

Different network services are not necessarily mutually exclusive. For example, a station running SatNOGS could pipe received data into another network, such as GENSO.

There are a couple of limitations in SatNOGS. Firstly, the output data is either in a in a lossy .ogg audio format or in binary files. Preferably there should be an option for raw IQ samples or lossless audio, although this requires a lot of storage and data transfer capacity. IQ samples are important for example in the radio channel research mentioned previously. Secondly there is currently no support for live operation, data is processed and distributed after the pass is over. Another issue is the number of stations and the hardware they employ. Particularly at GHz range frequencies the coverage is low, which could be a problem for AMOS-Sat. SatNOGS is open source, so if these problems are blocking a potential application, the user can submit their own fixes. For instance by providing more open source designs for GHz range stations, making them easier to adopt.

To further evaluate SatNOGS, the NUTS ground station is set into service as a network node. SatNOGS client must be built and installed on a computer running linux. To quickly test the system it is set up using an RTL-SDR [27], which is covered in the beginners guide [28]. Later this is switched to an USRP2.

Ubuntu is used, rather than Fedora which the beginners guide suggests. This is due to the author being more familiar with the Ubuntu environment. To make the system work under Ubuntu some modifications are required, detailed build instructions are found in appendix C.

Approximately 200 passes are tracked and recorded using SatNOGS. The data is available online [29]. One example of decoded satellite data is seen in figure 3.20.

For the NUTS and AMOS-Sat projects, SatNOGS is an interesting ground station service that has the needed basic feature set. The system is open source and by contributing to the project, this feature set can be expanded. SatNOGS has also been used to uplink to a CubeSat operating in the 430 MHz amateur band. A ready solution with flight heritage makes it particularly interesting for the NUTS project.

3. Build and verification of a VHF/UHF ground station

The upcoming AMOS-Sat project at NTNU will require a ground segment. To get more experience with ground station operation, NTNU needs to have an operational ground station. Focus is put on verification methods for ground stations, and how they tie into system performance.

The ground station for the NUTS project is finalised and put into service as a networked ground station node. This chapter details the Radio Frequency (RF) and mechanical portions of the setup. Many of the ground station components were already available from previous work [30], such as antennas, rotors, LNAs and SDRs. Initially these components were partially integrated and the system was not tested.

First the station setup is presented. Section 3.2 holds the methods for ground station verification. The results and discussion are presented in section 3.3.

3.1. Station setup

An amateur radio VHF/UHF satellite tracking ground station is set up to have full transmit (TX) and receive (RX) capabilities. The station is based on an SDR platform. A simplified block schematic is seen in figure 3.1. In this section a summary of the ground station is presented.

Appendix A contains a troubleshooting guide for station errors.

3.1.1. Software defined radio

This ground station setup is intended to be compatible with several SDRs. Currently it is implemented using two USRP2 [31] devices with WBX-40 daughtercards (radio frontends) [32]. One USRP is dedicated to the VHF band and the other is dedicated to the UHF band.

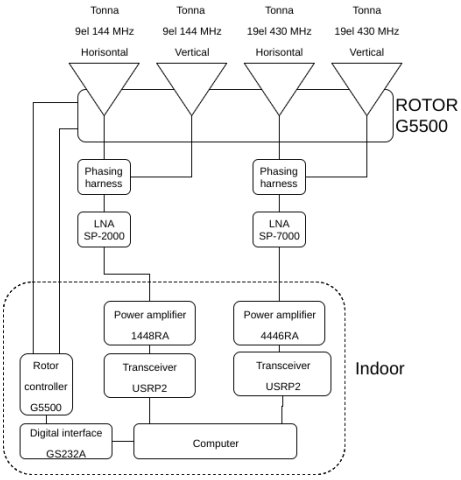

Figure 3.1.: Simplified block schematic of Gløshaugen site RF configuration.

Figure 3.2.: Crossed yagis for 144 MHz and 430 MHz at the Gløshaugen site.

The main drawback of the USRP2 is that the product is End-of-Life. This is not a large problem, since gnuradio [19] in combination with the USRP hardware driver (UHD) [33] is used as the software interface. Both gnuradio and UHD allow for writing largely hardware agnostic code. Should the SDR break in the future, it will be possible to replace it with a newer version or brand.

To improve the frequency stability and provide a common time reference, a Global Positioning System Disciplined Oscillator (GPSDO) is used. Cheng [34] describes that the GPSDO is a low-cost solution for highly accurate frequency reference in applications that have access to GPS signals. The GPSDO is a BG7TBL, which is characterised by Miles [35]. Frequency (10 MHz) and time reference (1 pulse per second (PPS)) signals are connected to each USRP2. To ensure minimum phase and time delay between USRPs, 10 MHz and 1 PPS distribution cables are made equally long.

3.1.2. Power amplifiers

The ground station is required to support uplink and downlink on both VHF and UHF amateur radio bands. SDRs often have low output powers in the 1 mW to 100 mW range [31][36][37]. In order to meet this requirement, amplifiers are installed to bring up the output power from the SDRs.

Each USRP is dedicated to a specific frequency band. The VHF USRP is connected to a TESystems 1448RA power amplifier, and the UHF USRP is connected to a

TESystems 4446RA power amplifier. The 1448RA amplifier requires a drive power of 0.25 to 0.5 W, and will deliver 160-200 W output power. The 4446RA requires a drive of 0.1 W and delivers 80-100 W output power. [38]

WBX-40 delivers between 1 mW and 100 mW of drive [39], so an intermediate stage is needed. While it seems like the intermediate stage could be dropped for the UHF USRP, WBX-40 will distort transmitted signals significantly when the output power is near the max level [32]. USRP power output is lowered to reduce distortion, and an intermediate stage is added.

The intermediate stage is provided by an additional module from the manufacturer. This module adds an internal intermediate stage as well as RF-sensed Receive/Transmit (RX/TX) switching. The alternative to RF-sensed switching is providing a transmit indication signal from the SDR. This signal can then be used to turn on/off relays. This would require modifying the firmware of the SDR, making it harder to replace the SDR if it should break in the future.

Power is supplied to the amplifiers via a RIGrunner 8012 [40] fused 13.8 V divider. If one of the amplifiers should malfunction and draw too much current, its fuse will blow. Since the main power supply does not go down, the other services can continue. The main power supply is an Astron RM-60M-220V [41] that will deliver 55 A 13.8 V.

The output of the amplifiers is connected to a 30 m run of low loss 1/2" heliax[42] via a RG-213 [43] jumper cable. Jumper cables between USRPs and amplifiers are 1 m pieces of RG-213.

3.1.3. Low noise amplifiers

SP-2000 and SP-7000 [44] LNAs are housed in a cabinet on the antenna mast. Power is supplied via DC injectors on the UHF heliax line. RF-sense is also available for the LNAs: SP-2000 can handle 200 W RF-sensed power pass-through and SP-7000 can handle 100 W. The LNAs are connected to the antennas through a custom designed phasing harness.

Cables between the antennas and phasing harnesses are 7 m RG-213 [43]. RG-213 is also used for the jumpers between heliax and LNAs.

3.1.4. Antennas

The antennas are a Tonna 2x9 [45] for VHF and a Tonna 2x19 [46] for UHF. Each antenna has two separate feedlines, one for the horisontal polarisation and one for the vertical polarisation. They are connected to the LNA and phasing harness

cabinet by pairwise equal length cables. The antennas are seen in figure 3.2.

A Yaesu G5500 rotor [47] enables steering in azimuth and elevation. A GS232B computer interface [48] is used for communication with the ground station computer.

3.1.5. Phasing harness for circular polarisation

Klofas [49][50] surveys of CubeSat communication systems show that linear polarised antennas are used in nearly all applications. NUTS is also set to use a linear polarised antenna. Davies [51] explains that circular polarisation at the ground station is desirable to cope with Faraday rotation and satellite tumble. When receiving linear polarisation with Right Hand Circular Polarisation (RHCP) or Left Hand Circular Polarisation (LHCP) the signal will always be - 3 dB lower compared to receiving it with a perfectly matched linear antenna [52]. The signal is always -3 dB, regardless of the orientation of the incoming linear wave. This causes the effects of Faraday rotation and satellite rotation to be reduced.

Since there is no demand on whether the circular polarisation should be RHCP or LHCP, RHCP is arbitrarily chosen.

In order to create RCHP with the 144 MHz 2x9 Tonna yagi and 430 MHz 2x19 Tonna yagi at the Gløshaugen site, two phasing harnesses are made.

The signal is split in two equal components by commercial power dividers from Wimo [53]. The vertical antenna polarisation is connected with a phase delay of 90° relative to the horisontal antenna polarisation. This phase delay can come from a combination of two sources, mechanical offset and electrical delay with a phasing line. These connections are summarised in figures 3.3 and 3.4.

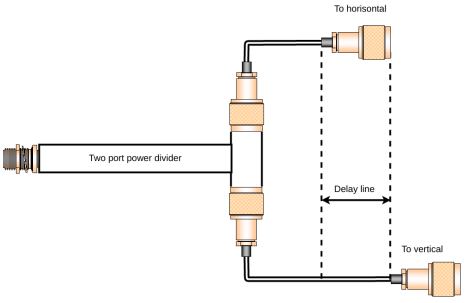

Figure 3.3.: Phasing harness for right hand circular polarisation.

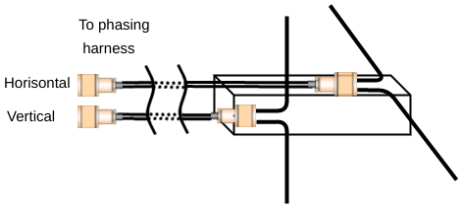

Figure 3.4.: Phasing harness connection to antenna. Polarisations are mechanically offset from each other.

The antennas in figure 3.2 are mounted so that the horisontal polarisation is in

Figure 3.5.: Inside the LNA and phasing cabinet.

front of the vertical polarisation for both VHF and UHF. The required phase line length after mechanical offset is given in an application note from the manufacturer as [54]

$$\Delta L_{440MHz} = 27 \cdot V_f \ [mm]$$

$$\Delta L_{144MHz} = 413 \cdot V_f \ [mm]$$

where V_f is the velocity factor of the coaxial cable. The additional phasing delay should be applied to the vertical polarisation. For convenience, the cables should be approximately 1 m long. Using RG-213 cable, which has a velocity factor of 0.66[43], the cut lengths are 1000 mm and 1272.5 mm for 144 MHz, and 1000 mm and 1017.8 mm for 430 MHz.

In order to have access to each polarisation without having to lower the mast, the harnesses are mounted inside a cabinet on the antenna mast. A connection diagram for this cabinet is seen in figure 3.6. The installed phasing harnesses is seen in figure 3.5.

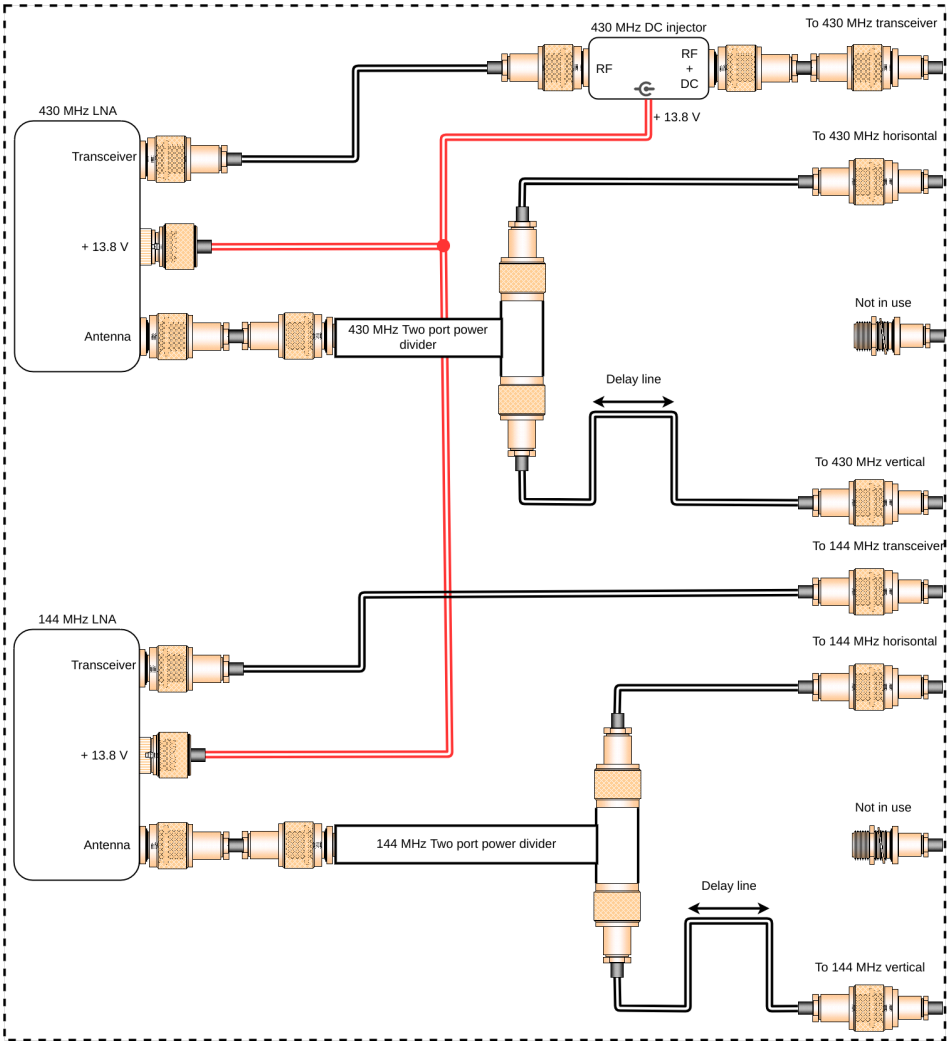

Figure 3.6.: Connection diagram for LNA and phasing harness cabinet at antenna mast.

3.1.6. Rack mounting

Integrating the ground station in a tidy way that is well documented is essential for continued operation. General maintenance and repair is made easier by rack mounting, making connection diagrams, and labelling all connections.

The rack is a 19" rack that is 20 rack units (20U) high and 600 mm deep. Rack layout is seen in figure 3.7. Figure 3.8 further elaborates on the DC, RF and rotor

connections. Due to long lead times, the amplifiers are not scheduled for delivery until mid-July, therefore they are not yet mounted in the rack.

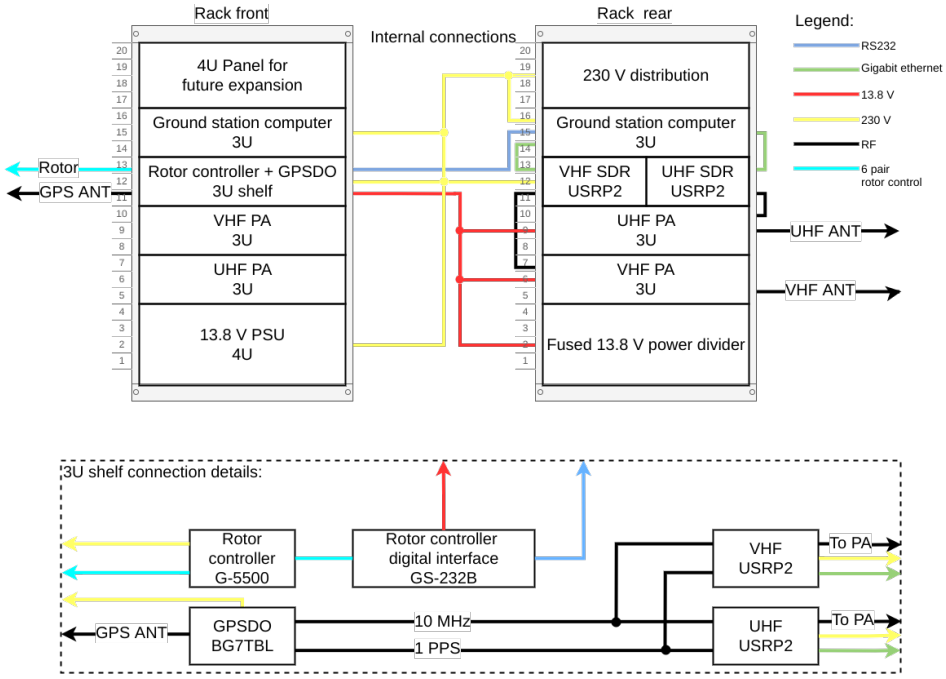

Figure 3.7.: Layout of the NUTS ground station rack.

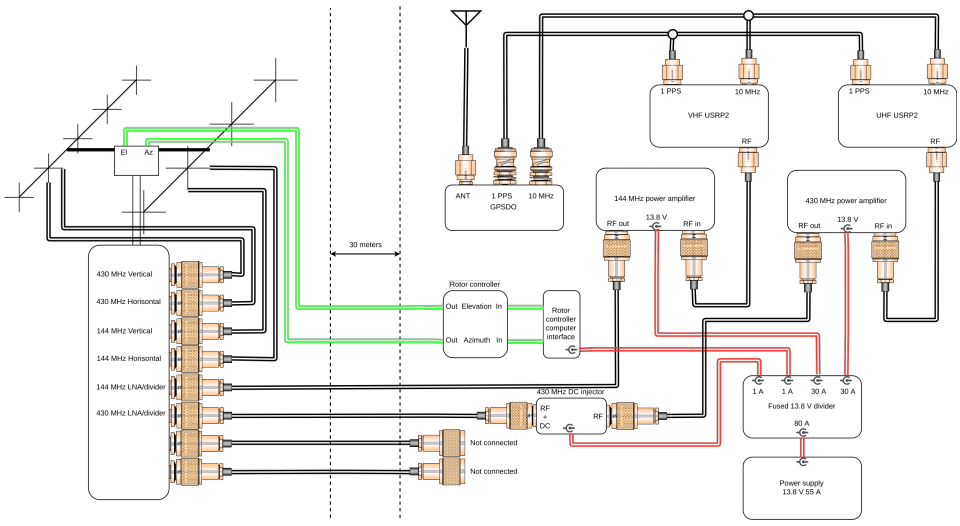

Figure 3.8.: Details of DC, RF and Rotor connections for the ground station.

3.2. Verification methodology

It is important to thoroughly test the system to ensure that it is working as intended before it must support critical missions. Having the ground station work with minor/no outages during the satellite mission is very important.

To achieve this the system must be tested and verified. To illustrate how the verified values affect the end result a link budget is calculated.

In this section the verification of the Gløshaugen ground station is described. To provide comparison, some of the components from the local student amateur radio club are also included. The amateur radio station is referred to as the Samfundet site, the setup of this station is described in section 4.2 in the earlier project report [30].

3.2.1. Antenna patterns

To better understand how the antennas perform, the antenna pattern is helpful. NTNU does not have facilities for measuring antenna patterns for frequencies below 1000 MHz, so another method is devised.

On top of a mountain approximately 20 km away from the two ground station sites there are two amateur radio beacons. These two beacons, LA2VHF and LA2UHF, transmit a Morse code sequence followed by a 10 second long carrier transmission in the 144 MHz and 430 MHz band, respectively. By rotating the antennas at the two sites and recording the signal strength during the 10 second carrier transmission a rough antenna pattern may be derived.

To get antenna patterns some assumptions must be made. First, the beacons are considered point sources. In reality they are not point sources, but horizontally polarised yagi antennas pointing northwards (towards the two sites). The beacons are also considered to be level with the two sites. Figure 3.9 makes this seem like a larger assumption than it actually is, the elevation angle between the Gløshaugen and beacon site is only $2°$. The elevation is kept at 0 degrees to make the measurement more symmetrical with regards to local ground planes. As the beacon antenna is horizontally oriented only measurements in the E field are made.

3.2.2. Low noise amplifier

A simple way to check if Low Noise Amplifiers (LNA) are working, is to turn on the power supply with a multimeter inline. The multimeter should then be able to read that the LNA is drawing the amount of current specified in the datasheet. By

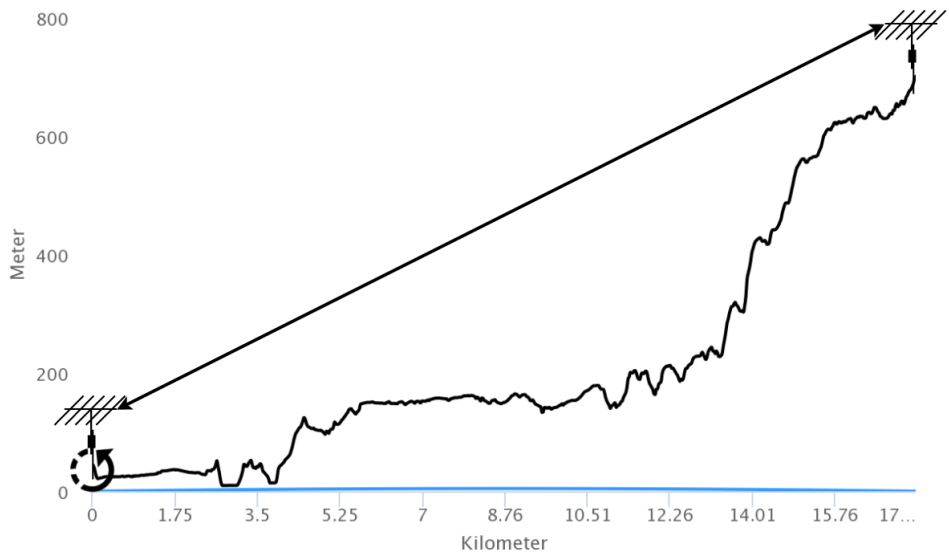

Figure 3.9.: Height map between one of the two stations (to the left) and the beacons (to the right) for the antenna pattern experiment.

toggling on and off the power to the LNA there should be an observable increase of the noise floor at the receiver compared to when the LNA is off.

To get numbers for SP-2000 and SP-7000 LNAs [44] to use in the link budget, more measurements must be done. For comparison the same measurements are also applied to SP-200 [55] and SP-70 [56] LNAs from the Samfundet site.

For all measurements an Aim-TTi EL302Tv precision power supply [57] is used to power the LNAs.

Noise figure and gain analysis

Using the FSV-K30 option [58] on a R&S FSQ signal analyser [59] with a HP 346B [60] noise source, the gain and noise figure of the SP-200, SP-2000, SP-70 and SP-7000 LNAs are measured. The measurement setup is seen in figure 3.10. The measurements are done at room temperature and the signal analyser is re-calibrated to the noise source every time the frequency range is changed. For thermal stability the equipment is left on for an hour before starting measurements.

LNA gain is adjustable by tuning a potentiometer. Each LNA is tested for three cases; maximum position, middle position and minimum position.

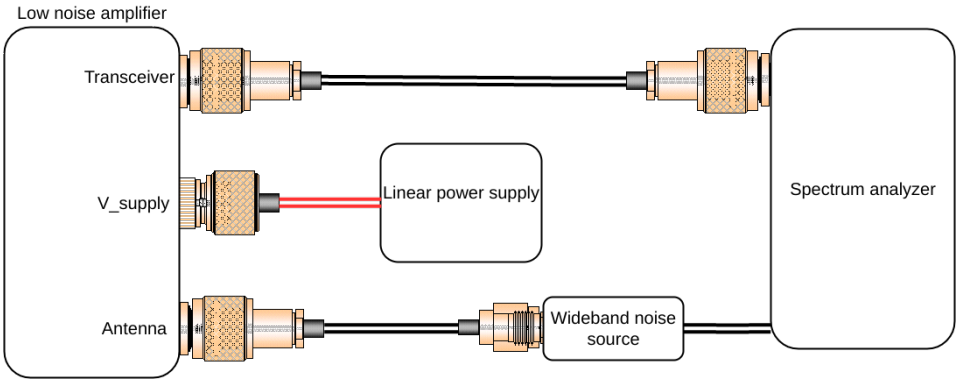

Figure 3.10.: Setup for gain and noise figure measurements on low noise amplifier(s).

Linearity analysis

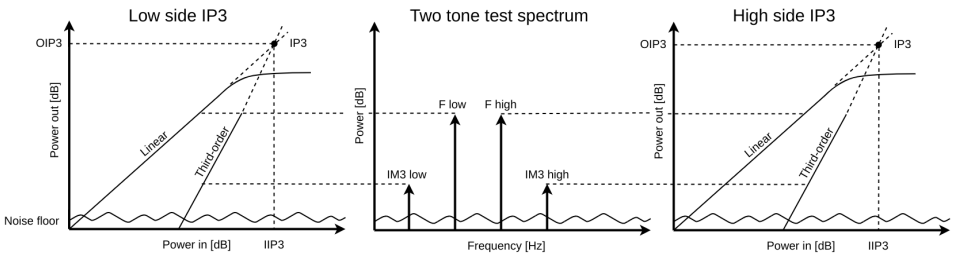

Figure 3.11.: Relation between two tone test for intermodulation products and high/low third order intercept points.

The n-th order intercept point (IPn) is where the n-th order intermodulation-product crosses the linear axis [61]. This is commonly used as a measure of linearity for non-linear devices, where a higher IPn value is better. Since our devices are highly linear, the measurement is noise floor limited beyond third order intercept (IP3).

By setting up a two-tone test, intermodulation 3rd order products will be generated in any non-linear device. These products can be found at $F_{high} + F_{spacing}$ and $F_{low} - F_{spacing}$. Using the level of these intermodulation products, output IP3 (OIP3) and input IP3 (IIP3) may be calculated as illustrated in figure 3.11. The third order intercept point is located at the intersection between the linear line and the third order line. In the logarithmic domain this may be mathematically expressed as:

$$P_{fundamental} + X = P_{IM3} + 3X.$$

Solving for X gives output referred location of the third order intercept point

$$OIP3 = \frac{P_{fundamental} - P_{IM3}}{2}.$$

Since the power difference between the output and the input is gain, the input referred third order intercept point can be found

$$IIP3 = OIP3 - Gain.$$

There is no guarantee that the low and high intermodulation power is equal, so low and high side OIP3 and IIP3 must be calculated.

IP3 measurement for mid-level of potentiometer is done right after NF and gain measurement to ensure that these occur at the same level.

Two-tone measurement is performed with 100 kHz spacing generated from a R&S SMU 200A signal generator [62] that is connected to the device under test. The resulting distortion is measured by a R&S FSQ 40 signal analyser [59]. Inherent test setup distortion is measured for all frequency ranges, but intermodulation products were buried in the noise floor for generator output power of -37 dBm per carrier. The powers of fundamental and intermodulation frequencies are read out at: 144.85 MHz, 144.95 MHz, 145.05 MHz and 145.15 MHz for the SP-2000 and SP-200 LNAs. For the SP-7000 and SP-700 LNAs the frequencies are: 434.85 MHz, 434.95 MHz, 435.05 MHz and 435.15 MHz.

Saturation

In presence of a strong transmitter the LNA might saturate. If this happens it may be necessary to add filtering to attenuate the saturation source.

The measure of how much input power an amplifier can take before spurious emissions are generated is the Spurious Free Dynamic Range (DR_f). DR_f is given as the magnitude relation between [61]

$$DR_f = \frac{P_{fundamental}}{P_{IMD3}}$$

If the goal is to measure signals that are at the noise floor, the signal that will induce detrimental spurious behaviour is located at DR_f dB over the noise floor.

It is important to note that DR_f is measured at a specific frequency spacing, and

that DR_f is typically lower for close spacing [63].

Insertion loss

To properly evaluate the uplink budget, the insertion loss of the LNAs in bypass mode must be known. This is measured by a R&S ZNB 8 Vector Network Analyser (VNA) [64]. Calibration is done with a HP 85052B calibration kit [65].

3.2.3. Phasing harnesses

The setup in figure 3.12 is used to measure the Scattering parameters (S-parameters) of the power dividers. An ideal two port power divider has a S21/S12 that is -3 dB [66]. Anything beyond this may be considered insertion loss. A R&S ZNB 8 VNA [64] is used to perform the measurement. Calibration is done with a HP 85052B calibration kit [65].

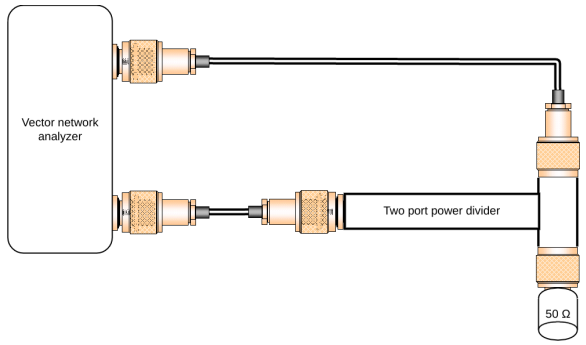

Figure 3.12.: VNA measurement of Wimo power dividers. Common port connected to VNA port 1, one divided port connected to port 2, the other is terminated in 50 Ω.

A simulation of an ideal quarter wave transformer divider is made in Keysight Advanced Design System (ADS)[67] to see how the performance compares to the measured devices. The simulations are seen in figure 3.13. Passive three port splitters/combiners can never be both lossless and matched at all three ports[66]. The simulation gives more insight into the inner workings of the splitter, which is seen to be input matched, lossless and reciprocal, but has unmatched outputs.

To measure the phase offset a R&S SMU 200A signal generator[62] is connected to the common port of the phasing harness, and each output is connected to an Agilent MSO9254A[68] oscilloscope. The oscilloscope has BNC-male connectors,

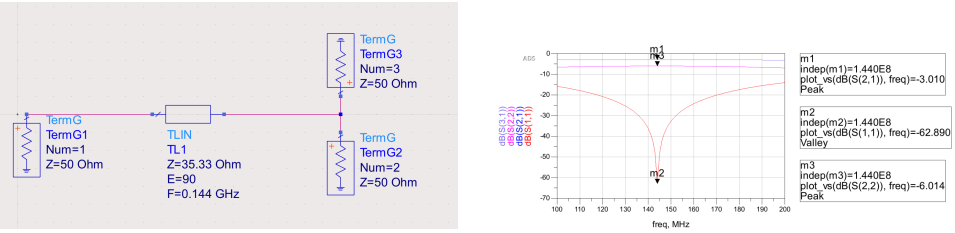

(a) Schematic for ideal divider.

(b) S11, S22 and S21 for the ideal divider.

Figure 3.13.: Quarter-wave coaxial transformer divider simulations.

so a N-female to BNC-male transition is needed. The two transitions are from the same brand, and should not cause any significant phase offset.

As will be seen in the results, the phase mismatch for the fabricated cables is too large. The same cable fabrication method is also used for the jumper cables between the phasing harness and the antenna, so another method to measure phase is devised.

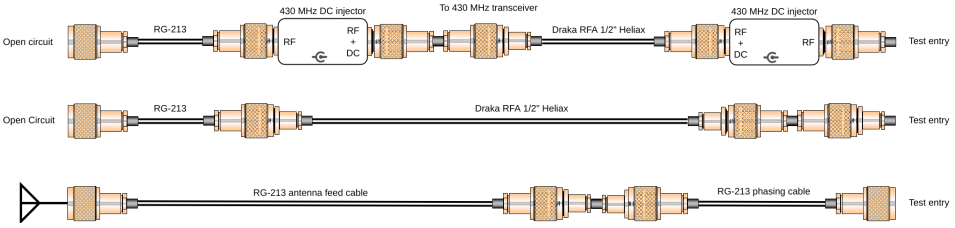

Figure 3.14.: Cable topologies for distance-to-fault length measurements.

By using the distance-to-fault (DTF) option FSK-41 on a R&S FSH8 spectrum analyser [69], the precise length to a fault in a coaxial line can be measured. DTF works by transmitting a pulse over a frequency sweep and then listening to echoes from radiating corners, mismatched points, open ends and so on. The device is calibrated in the same way as a network analyser, with one important addition. In order to accurately measure length, the DTF instrument needs to know the velocity factor and attenuation of the coaxial cable that is being measured.

Once the length is known, cable-induced phase difference can be calculated from the cable length using the velocity factor.

By measuring with a sweep from 1.5 GHz to 2.5 GHz the lengths between the different cable assembly topologies seen in figure 3.14 are measured. The antenna terminated topology is repeated four times to measure all antenna feed lengths. Since the antenna is not resonant for all frequencies between 1.5 GHz and 2.5 GHz the antenna input will reflect, causing a fault to be detected. For the open circuit

topologies, the FSH8 is set to calculate using a Draka RFA 1/2" [42] cable as reference. This will cause a slight mis-measurement as there are short sections of RG-213 and DC injectors on the 430 MHz line. Antenna terminated topologies use RG-213 [43] cable as reference.

This measurement could also be performed by a network analyser. This method might give a better idea of the insertion loss. However, the measurement is very cumbersome to perform as the test cables would have to be the same length as the tested cables (30 m). Furthermore the antenna mast would have to be brought down.

Since the cable losses are included in the link budget, the cables between the cabinet and amplifiers are also measured. The fault is created by disconnecting the RG-213 patch cable that goes to the LNA output port. When adding these figures to the link budget 1-2 dB should be added to account for connector and DC injector losses.

3.2.4. Power amplifier characteristics

The 1446RA and 4446RA amplifiers are used for uplink from the ground station. Due to long lead times from the manufacturer these are not scheduled for delivery until mid-July. In this section the steps for measuring the characteristics of these amplifiers are given.

The 1448RA amplifier requires a drive power of 0.25 to 0.5 W, and will deliver 160-200 W output power. The 4446RA requires a drive of 0.1 W and delivers 80-100 W output power. Since the USRP SDRs deliver between 1-10 mW [32] an intermediate stage is needed. This intermediate stage is provided by an additional module from the manufacturer. This module adds an internal intermediate stage as well as RF-sensed transmit/receive switching. This additional module should allow drive levels as low as 5 mW.

Measurement setup and safety evaluation

Measuring on high power equipment requires certain precautions, as there are a number of health and safety hazards that may be encountered. In particular, it is important to reduce the risk of electrical shock and RF burns. It is also important to keep the power levels at the instrument ports within specifications.

The measurement consists of three scenarios depicted in figure 3.15. The amplifiers are powered by a +13.8 V 55 A Astron power supply [41].

The first measurement is a dry-test. The dry-test is a setup verification, to ensure

that the measurements can be done without risk to measurement equipment or people. In this test only passive components are used at critical junctions.

Ensuring good connections is vital for safe measurements. RF-connectors should be tightened by torque wrench to ensure contact. False connections can lead to large reflections that may damage the amplifier. Additionally, these connections can cause spark gaps, which may be dangerous for the operator.

Cables must be selected to ensure proper power handling. The coaxial cable between 1448RA and the high power attenuator is of particular importance, and should be able to handle in excess of 200 W continuous power at target frequency. DC-cables should be selected so that they can handle at least 40 A, somewhat higher than the specified current draw of the amplifiers at 26 A (UHF) and 29 A (VHF).

Attenuators are important for making this setup safe for the measurement equipment. Reducing the output power from the amplifier from a max around 53 dBm to something below -20 dBm is the primary concern. Particularly, the first attenuator should be able to handle 200 W continuously and exhibit low input reflectivity across the frequency range in order to keep reflected power to the amplifier to a minimum.

Before proceeding with measurement steps 2 and 3, the following characteristics must be observed:

- Before setup, check S-parameters of measurement components.
- Current draw of amplifiers should stay stable over 10 minutes.
- Power readout from power meter is at expected level and should not fluctuate significantly over 10 minutes.
- Check thermal levels using a thermal camera. Particularly the high power attenuator and amplifier radiators are expected to have a high thermal profile. If any components get excessively hot, double check connections and test again.

In measurement scenario 2 the spurious performance and compression of the amplifiers will be tested. The spurious tests should show that the amplifier behaves within the legal limit, and does not distort the transmitted signal. The tele-regulatory authority requires that all transmissions in the VHF and UHF amateur radio band not cause radiated spurious emissions that are above -26 dBm for frequencies above 30 MHz [12].

The output power from the amplifier should not exceed 53 dBm for the VHF amplifier and 50 dBm for the UHF amplifier, as this exceeds the RF sensed power limit for the SP-2000 and SP-7000 LNAs [44].

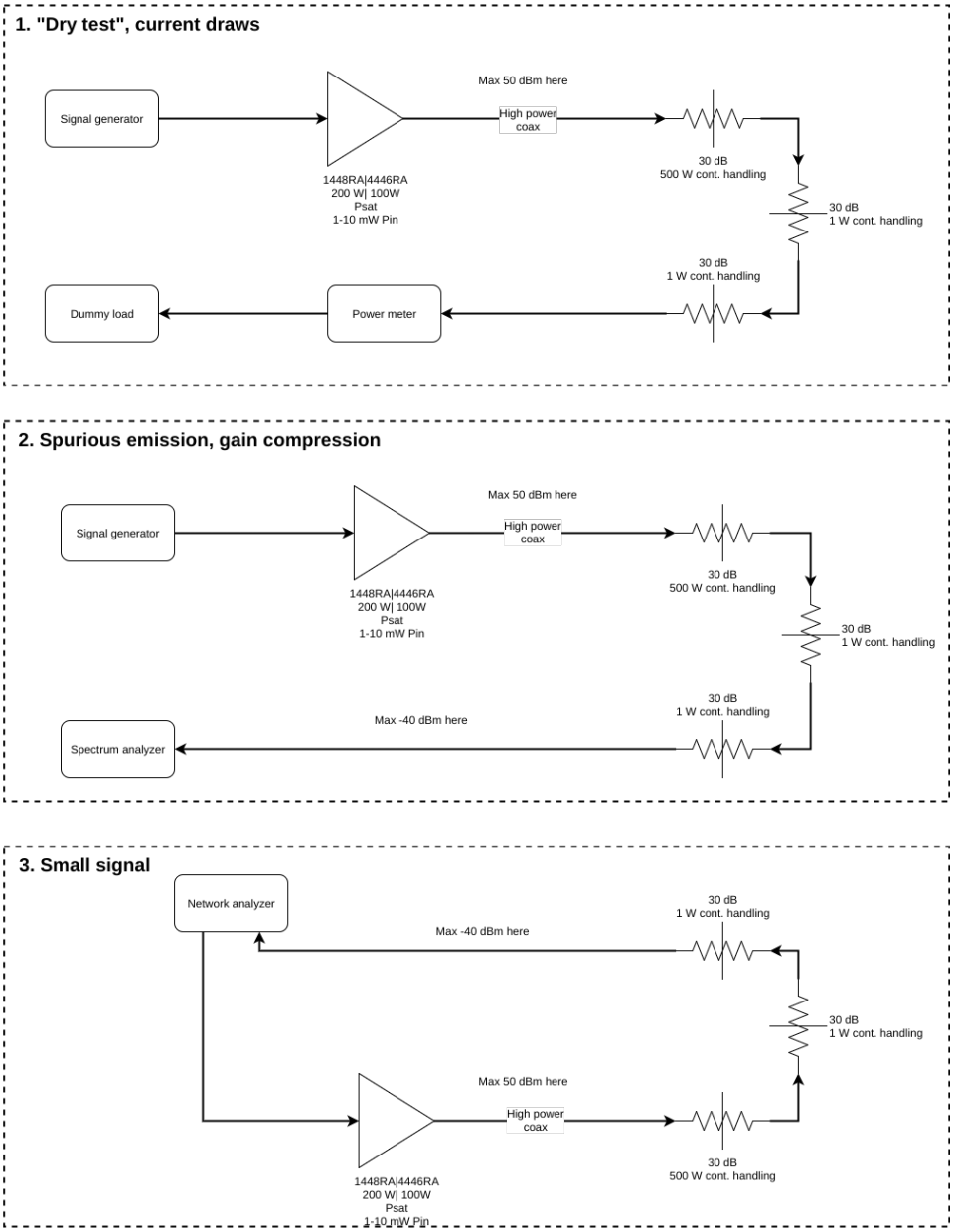

Figure 3.15.: Three test cases for measuring the performance of TE Systems 1448RA and 4446RA amplifiers.

Finally, in measurement scenario 3, the small signal characteristics of the amplifier will be addressed. S21 should be measured at three different power levels: linear

region, knee region and deep compression. The power levels are determined from the results of measurement scenario 2. Input and output reflectivity should also be measured.

Expected results

Since the amplifiers are not yet delivered, it is not possible to measure them for this report.

The amplifiers are expected to deliver 100 W and 200 W output power for the UHF and VHF bands, respectively. These output powers are likely to occur at some type of compression so a slight backoff of 1 dB or so may be necessary. The IP3 values of the amplifiers are expected to be much lower than the LNAs, perhaps as much as 10-15 dB.

3.2.5. Link budget

NUTS link budget should show that the ground station is able to support the satellite after launch, using the verified numbers from the methods above. If there are any major discrepancies, action must be taken to ensure the link will work.

In this section the various terms in the budget are described.

Path loss

There are two approaches when calculating path loss. The first is to estimate the path loss to consist of only a free space path loss (FSPL) component, and then add inn models for atmospheric and ionospheric losses. The second is to use a path loss model. Here the first approach is chosen.

Friis equation is used to calculate FSPL [61]

$$FSPL\ [dB] = 10\log_{10}(\frac{4\pi df}{c})^2.$$

Where f is the frequency, c is the speed of light and d is the distance between transmitter and receiver.

Ionospheric effects

International Telecommunication Union (ITU) recommendation P.531-13 [70] details transiononspheric communications. Particularly two phenomena are likely to affect LEO communications, those are ionospheric scintillation and absorption. Basu [71] explains that ionospheric scintillations are phase and magnitude fluctuations on a signal that occur when the variation of intersected Total Electron Content (TEC) is high. Absorption is a similar phenomenon, but here some of the signal power is absorbed by plasmas in the ionosphere [51].

As seen in figure 5 in [70] the scintillation index (S4) for VHF is generally higher than for UHF. S4 is chosen at a moderate level of 0.5 for UHF, giving peak-to-peak scintillation fluctuation of 11 dB. For VHF a high level of 0.9 is chosen, giving a fluctuation of 24 dB. This fluctuation can be both constructive and destructive. As an estimate, half the peak-to-peak value is modelled as loss in the link budget.

Basu [71] shows that scintillations are sporadic phenomena that occur in conjunction with solar spots. In 2017 there is a low number of sunspots [72], but solar activity is likely to increase again during the duration of the mission. To be conservative, a high estimate for scintillation is chosen. Sreeja [73] shows that during a solar maximum the scintillation occurrence for a high latitude station (Brønnøysund) can be as high as 30% at certain times of day for a L-band receiver. Outside peak-hours the scintillation occurrence is on the order of 0 to 5 %.

The second phenomenon is absorption, and particularly polar cap absorption for high latitude ground stations. Davies [51] study on propagation impairments due to the ionoshere indicates that this value is around 5 dB for VHF and 0.2 dB for UHF. This is a little high compared to the numbers given in ITU recommendation P.531-13 [70]. However, P.531-13 also mentions that polar cap absorption may exceed 5 dB during solar flares at high latitudes, albeit for a much lower frequency than what is used in the ground station.

Both of these phenomena depend on intersected TEC [51], and will vary over a satellite pass. This means that the ground station may experience scintillations while tracking.

Atmospheric effects

ITU also has a recommendation for attenuation caused by atmospheric gases[74]. Since atmospheric attenuation is caused by gases, it increases with lower elevation angle. More atmosphere, and conversely more gases, are intersected. Gas density becomes insignificant at 30 km altitude. At 10° elevation the intersected atmosphere is roughly 200 km. Multiplying this with $3 \cdot 10^{-3}$ dB/km (from figure 1 in [74]) gives an approximate atmospheric attenuation of 0.5 dB.

Rain attenuation is not assessed as it is negligible below 1 GHz according to ITU-R P.838-3 [75].

Pointing loss

NUTS features attitude control through a magnetourqer [76] that will attempt to align the satellite along the earth-satellite axis. The amount of loss caused by misalignment is determined by how accurate the attitude control is. Circular polarisation means that rotation along the earth-satellite axis will not cause problems, as illustrated in figure 3.16.

Existing systems provide attitude control that is better than 10° [77][78]. The antenna pattern for NUTS is not yet determined, but it is likely to largely resemble a dipole, which has a 3dB beamwidth of approximately 80° [52]. This means that if attitude control is successful, the satellite pointing loss will be small, on the order of 0.1-0.2 dB.

Pointing loss also occurs on the ground station side, partly because of boresight calibration error, but mostly because of aged two-line-elements set (TLEs). TLEs are used to estimate the satellite position. When the TLEs are aged, the satellite position prediction will give an angular error as shown by Hinckley [79]. Assuming a TLE age of 4 days, the angular error will be approximately 10°. By comparing this to the antenna patterns in section 3.3.1 the pointing loss of the tracking ground station can be derived.

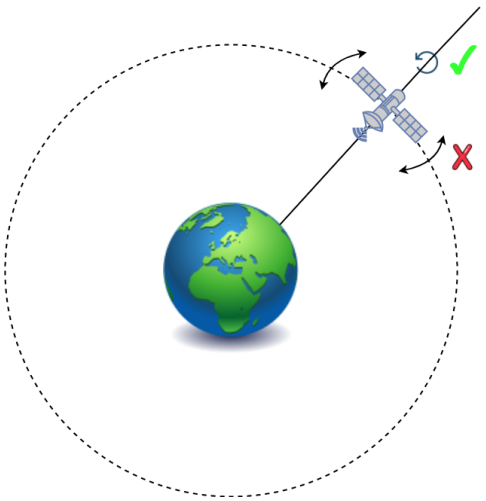

Figure 3.16.: Rotation around earth-satellite axis is will not cause pointing loss, but any other rotation will.

Doppler shift

Information on satellite position and velocity is used to correct for the large Doppler shift caused by the satellite speed. When the TLE used to calculate this is inaccurate or outdated the Doppler shift correction will also become inaccurate.

Comparing figures 13 and 15 in Murotas [80] work on land mobile GMSK channels, the BER increases immensely for small Doppler shifts. In the link budget the numbers from the static scenario is used, but it is apparent that the link budget becomes inaccurate once Doppler shifts occur. As long as there is no real time demand, Doppler shift correction can be performed during post-processing [81]. This is one of the advantages of an SDR based platform, as it allows sampling a large enough bandwidth to get the signal including maximum Doppler shifts.

On the satellite side, a phase-locked-loop (PLL) is responsible for correcting for the Doppler shift.

3.3. Results and discussion

In this section results from the measurements, calculations and estimations, as described in section 3.2, are presented and discussed.

3.3.1. Antenna patterns

In figure 3.17 the results from the antenna pattern measurements are compared against the patterns given in the datasheets for the respective antennas.

Both 3.17a and 3.17c deviate from the expected results between 120°and 20°. This may be because of strong reflections from a hillside that coincide with these angles. Another possibility is that the close proximity of the two antennas may cause mutual coupling which can effect the antenna patterns. This is unlikely as the lobes occur for the same angles for both antennas, and the geometry of the stack suggests that such errors should occur on opposite angles.

The pattern in 3.17e exhibits a squinting main lobe. One likely cause is the large ventilation aggregate that is installed right behind the antenna. A large backlobe can be seen between 288°and 340°, where the ventilation is located. Also note the axis-scaling of the expected results in figure 3.17f, which reduces the visual impact of the side-lobes.

The main limitation of this measurement is that it is not known whether a lobe is the result of the actual antenna pattern, or reflections in the nearby environment.

To amend this it is possible to set up a test signal in a different location, and see if the pattern changes significantly with a new measurement. If the pattern does not change, it is likely the actual antenna pattern that was measured. To perform these measurements, additional equipment would be required, which would have to be moved around to different sites. Due to these constraints, this measurement was not performed.

Overall, the antenna patterns for the Gløshaugen site have similar shape to what their datasheets indicate. There is some mis-match but the gain value should be similar to what is given in the datasheet.

3.3.2. Low noise amplifier

The results are presented in table 3.1. NF and Gain curves are found in appendix B.

Overall the LNAs have good measures with a max NF around 1.8 dB and OIP3 values higher than 33.5 dBm. However, the NF of the SP-2000 and SP-7000 LNAs are almost 1 dB worse than what their datasheets [44] specify. One possible cause is deterioration due to ageing. Somewhat surprisingly, and also contrary to the datasheet, the noise figure is also consistently better for the highest gain setting. One possible reason for gain dependent NF is that NF only looks worse, but in fact is affected by the resolution of the measurement equipment, which is lower for lower gain [58]. The NF resolution is about 0.1 dB for 10 dB gain, and 0.01 dB for 20 dB gain.

To safeguard against saturation, an empirical observation is made to see that there are no overly strong signals in the passband. The strongest persistent signals that are found are the LA2VHF and LA2UHF beacons. These are far from the common satellite frequencies.

The band plans [82][83] dictate where different amateur radio activities should take place in the band. It reserves frequencies for satellite/space communications. This means that the only time the LNA would experience strong signals is when a local station is trying to uplink to the same satellite that is being tracked. This is such a rare case that it can safely be ignored. Since the band plan allocates such a large bandwidth, testing DR_f at 100 kHz is adequate.

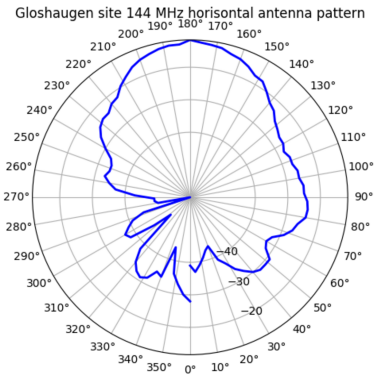

(a) Measured E field pattern for horisontal polarisation of 144 MHz Tonna 2x9 antenna.

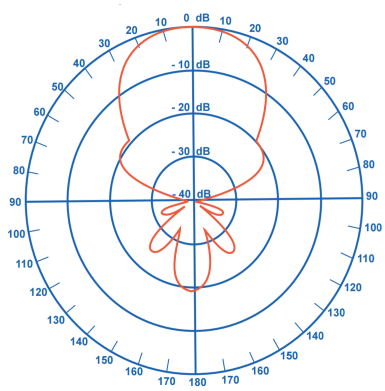

(b) E field pattern from Tonna 144 MHz 2x9 element datasheet[45].

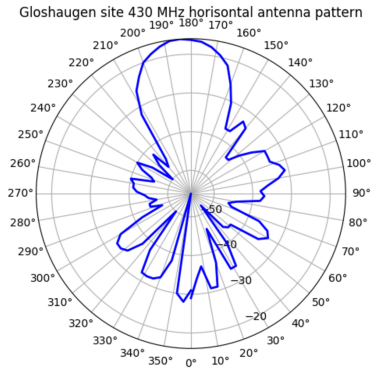

(c) Measured E field pattern for horisontal polarisation of 430 MHz Tonna 2x19 antenna.

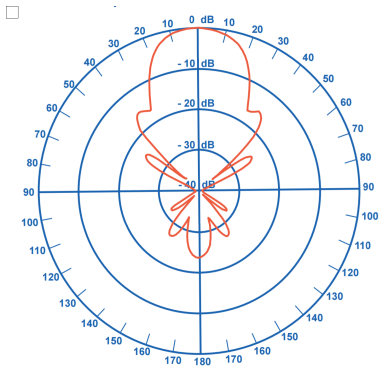

(d) E field pattern from Tonna 430 MHz 2x19 element datasheet[46].

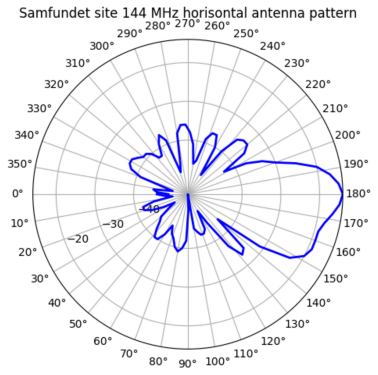

(e) Measured E field pattern for 4 bay array of 144 MHz 12 element LFA antenna.

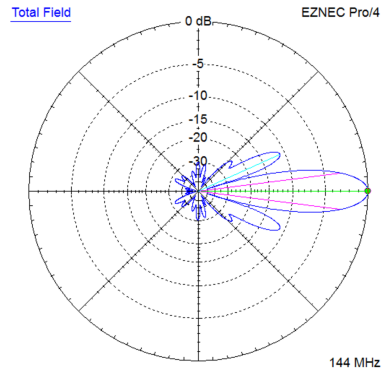

(f) Simulated E field pattern for 4 bay array of 144 MHz 12 element LFA antenna.

Figure 3.17.: Comparisons of measured antenna pattern to datasheet or simulated values.

Table 3.1.: Measured LNA characteristics.

Device under test	Test frequency [MHz]	NF [dB]	Gain [dB]	P_high [dBm]	P_low [dBm]	IM3_low [dBm]	IM3_high [dBm]	OIP3_high [dBm]	OIP3_low [dBm]	IIP3_high [dBm]	IIP3_low [dBm]	DR_f high [dBm]	DR_f low [dBm]	Bypass insertion loss [dB]
SP-2000 - medium gain	145	1.90	23.08	-25.07	-25.23	-89.1	-92.5	33.72	31.94	10.64	8.86	67.43	63.87	0.09
SP-2000 - high gain	145	2.01	13.91	-20.79	-20.95	-84.5	-87.8	33.51	31.78	19.6	17.87	67.01	63.55	0.09
SP-2000 - low gain	145	1.92	18.58	-29.78	-29.95	-93.8	-96.6	33.41	31.92	14.83	13.34	66.82	63.85	0.09
SP-200 - medium gain	145	0.40	20.50	-26.53	-26.67	-98.6	-98.4	35.92	35.97	15.44	15.47	71.87	71.93	0.06
SP-200 - high gain	145	0.57	12.73	-22.64	-22.79	-95.5	-95.6	36.48	36.35	23.75	23.63	72.96	72.71	0.06
SP-200 - low gain	145	0.36	16.88	-30.75	-30.91	-102.6	-102.2	35.73	35.85	18.85	18.97	71.45	71.69	0.06
SP-7000 - medium gain	434	1.25	22.60	-26.79	-26.93	-102.2	-104.3	38.76	37.64	16.16	15.035	77.51	75.27	0.28
SP-7000 - high gain	434	1.84	12.23	-21.22	-21.34	-96.8	-98.9	38.84	37.73	26.61	25.5	77.68	75.46	0.28
SP-7000 - low gain	434	1.51	16.96	-31.3	-31.35	-106.8	-109.1	38.9	37.73	21.94	20.77	77.8	75.45	0.28
SP-70 - medium gain	434	0.68	22.13	-24.04	-24.1	-98.2	-102.1	39.03	37.05	16.9	14.92	78.06	74.1	0.17
SP-70 - high gain	434	1.22	12.72	-21.6	-21.64	-95.6	-99.4	38.9	36.98	26.18	24.26	77.8	73.96	0.17
SP-70 - low gain	434	0.78	19.59	-30.95	-31.0	-105.3	-108.5	38.8	37.15	19.18	17.56	77.55	74.3	0.17

3.3.3. Software defined radio

The RF performance of USRP devices and their daughter-boards are well documented. The daughter-board used in the ground station are WBX-40 [39] which has TX- and RX-figures that is found in [32].

Since the radio does not employ filtering on the RF outputs/inputs, it has large problems with spurious performance. Particularly, the unwanted harmonics have high levels. This will be revisited in section 4.3.1. External filtering will in many cases be necessary.

Saturation may also be an issue, however as discussed in the previous section it rarely occurs in this amateur radio band. Care should be taken by the operator to not increase the USRP gain so much that the receiver saturates.

The local oscillator (LO) will leak through the WBX mixer. To make sure that this does not interfere with reception or transmission the LO should be set at an offset [84].

3.3.4. Phasing harness

Power divider insertion loss is presented in table 3.2.

Table 3.2.: S-parameters for 144 MHz and 430 MHz power splitters from Wimo.

	144 MHz	148 MHz	430 MHz	438 MHz
S11 [dB]	-22.2	-23.0	-21.10	-22.13
S22 [dB]	-6.08	-6.05	-5.69	-6.0
S21 [dB]	-3.15	-3.14	-3.68	-3.74
Insertion loss TX/RX-Ant [dB]	0.15	0.14	0.68	0.74
S12 [dB]	-3.06	-3.03	-3.71	-3.81
Insertion loss Ant-TX/RX [dB]	0.06	0.03	0.71	0.81
S22 [Ω]	138.7+j34.1	143.7+j26.3	95.6+j70.6	120.4+j58.2

The S22 parameter for both dividers is very high. In this application it does not matter, since the receive path insertion loss is not excessively high. S11 for the measurement is approximately -20 dB, which is not as low as the -60 dB from the simulations. Finally the insertion loss is 0.14 dB for VHF and 0.71 dB for UHF. Accounting for real life loss this is within expectations, however the insertion loss for UHF is quite high.

The largest phasing length error from DTF measurement in table 3.4 is for 430 MHz, and corresponds to a 14° mismatch. This is much better than the 62.9° mismatch previously seen with the oscilloscope measurement in table 3.3. A 14°

Table 3.3.: Oscilloscope measured phase offset of 144 MHz and 430 MHz phasing harnesses.

	144 MHz phasing harness	430 MHz phasing harness
Target phase offset [°]	72.36	14.0
Measured phase offset [°]	9.4	1.5

Table 3.4.: DTF measured length and calculated attenuation for ground station cables. *: Attenuation calculated from [43] and [42] assuming entire length is composed of same cable.

	Length [m]	Calculated attenuation* [dB]
144 MHz Amplifier to LNA	33.78	0.89
430 MHz Amplifier to LNA	33.59	1.56
144 MHz LNA to horisontal	7.81	0.67
144 MHz LNA to vertical	8.079	0.69
430 MHz LNA to horisontal	8.016	1.28
430 MHz LNA to vertical	8.016	1.28
144 MHz phasing length target	0.273	N/A
144 MHz phasing length error	0.004	N/A
430 MHz phasing length target	0.018	N/A
430 MHz phasing length error	0.018	N/A

mismatch means that the polarisation will be slightly elliptical. At 14° the error is small enough to be discounted. For 62.9° mismatch the polarisation would be narrow elliptical, bordering on linear. [52]

To see that the phasing harness is working as expected, two passes of the same satellite are tracked and recorded. Since passes are very similar, they should see the same local reflections. Passes are taken quite far apart in time, so ionospheric conditions and satellite state are not the same.

Comparing the two passes in figure 3.18, the signal strength of the left signal is weaker than the peaks of the right signal. The left signal has a much more consistent power level. This is in line with the expectation from installing a phasing harness.

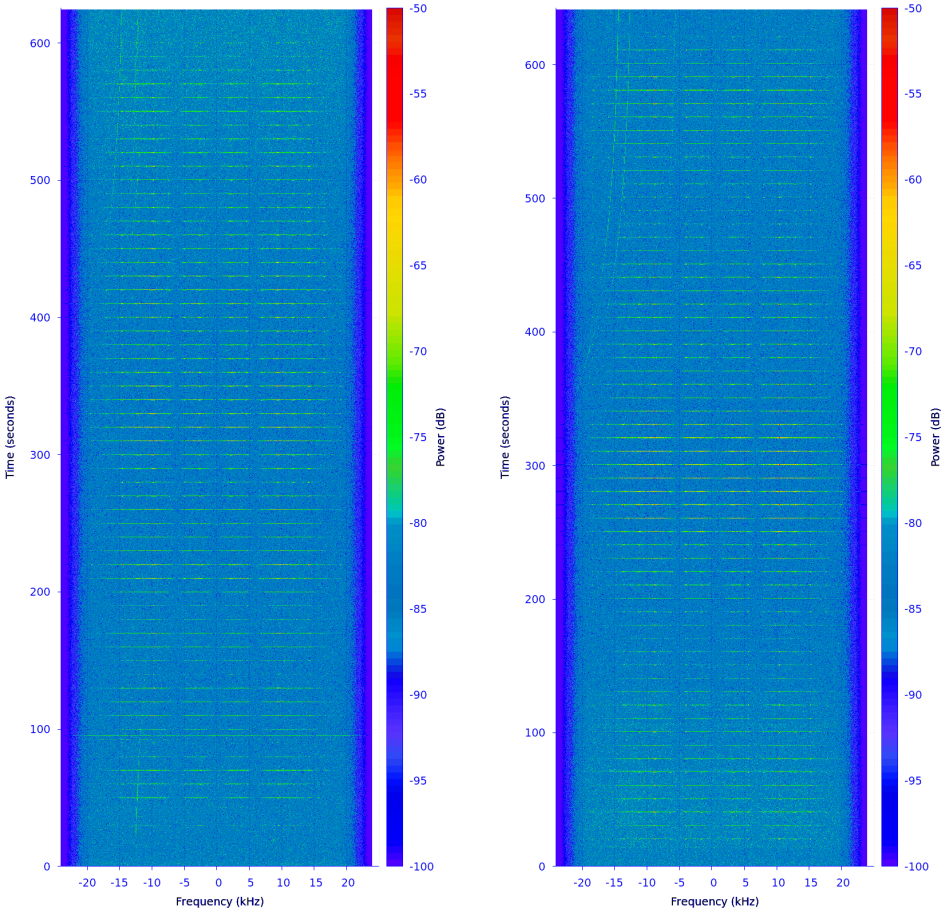

(a) Waterfall of Tianwang 1A pass with phasing harness. Rise azimuth: 205° Max elevation: 19° Set azimuth: 338°.[85]

(b) Waterfall of Tianwang 1A pass without phasing harness. Rise azimuth: 197° Max elevation: 23° Set azimuth: 339°.[86]

Figure 3.18.: Two passes similar passes of Tianwang 1A with and without phasing harness.

3.3.5. Tracking and decoding

As a final systems test, the ground stations are set up to track and decode data from a satellite. The 137 MHz National Oceanic and Atmospheric Administration (NOAA) weather satellites are chosen as they have frequent passes and are easy to decode by feeding recorded audio to WXtoImg [87]. The decoded data is seen in figures 3.19 and 3.20. Samfundet site audio is manually collected, while Gløshaugen site is gathered from SatNOGS.

The images are originally greyscale, but since the position of the satellite is known it is possible to apply map overlay and colour correction in post processing.

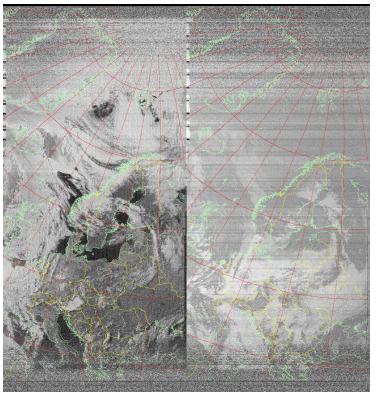

Figure 3.19.: NOAA 15 image with map overlay added in post processing, decoded from a pass over the Samfundet site.

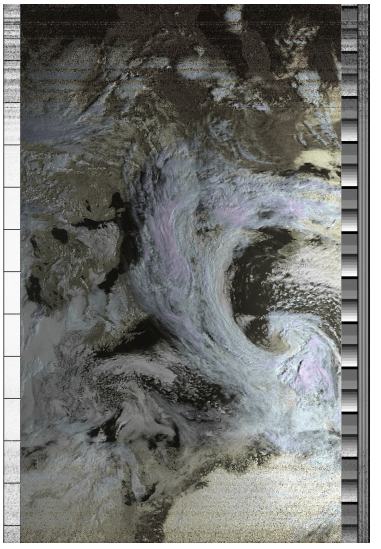

Figure 3.20.: NOAA 15 image with colour correction done in post processing, decoded from a pass over the Gløshaugen site.

3.3.6. Link budget

With the verifications made in the previous section, a link budget is calculated to show what satellites may be supported. Link budgets are presented in tables 3.5 and 3.6.

Parameters are defined at a 10° elevation angle, the lowest angle where the ground station has free sight of the horizon as measured by Stenhaug [88]. At such a low elevation angle, path loss is maximised. Further the intersected atmosphere and ionosphere along the path are also maximised. This means that if a satellite is supportable at this elevation, it is supportable at all higher elevations.

The satellite orbit is undecided, and many of the satellite figures are also unspecified. In order to guarantee that any realistic orbit height is supportable, a LEO orbit of 1000 km is chosen for calculations. Plooms [89] analysis of CubeSat orbit parameters shows that this height is higher than most recent CubeSat launches.

Frequencies are from the NUTS frequency allocation document [90] and bandwidths are the maximum given by the tele-regulatory authority [12].

For the uplink the link budget is calculated using sensitivity measures of the radio devices. Sensitivity is the lowest power where a given bit error rate for a given modulation can be supported [61]. This is mostly due to the VHF radio, Owl VHF, which states sensitivity in the datasheet [91]. The UHF radio for NUTS is not complete yet. To get an estimate for the link budget the sensitivity of another recent CubeSat, UpSat [21], is used.

On the downlink side, the sensitivity for the system is not readily available due to the unique combination of antennas, cables, LNAs and receivers. Since each component is characterised, the link budget can be calculated using the noise temperature approach from [61].

Table 3.5.: VHF and UHF uplink link budgets.

Uplink 437.305 MHz	**Data**	**Result**	**Unit**	**Source**	**Uplink 145.980 MHz**	**Data**	**Result**	**Unit**	**Source**
Transmitter					**Transmitter**				
Power out	49		dBm	PA output power, slight backoff [92]	Power out	52		dBm	PA output power, slight backoff [92]
Feedline loss	2		dB	Table 3.4 with connector loss	Feedline loss	1.5		dB	Table 3.4 with connector loss
LNA bypass loss	0.28		dB	Table 3.1	LNA bypass loss	0.1		dB	Table 3.1
Power divider loss	0.7		dB	Table 3.2	Power divider loss	0.1		dB	Table 3.2
Antenna jumper loss	2		dB	Table 3.4 with connector loss	Antenna jumper loss	1.5		dB	Table 3.4 with connector loss
Antenna gain	16		dBi		Antenna gain	13.1		dBi	
EIRP		60.0	dBm		EIRP		61.9	dBm	
Propagation					**Propagation**				
Orbit height	1000		km		Orbit height	1000		km	
Slant distance 10°	3000		km		Slant distance 10°	3000		km	
Free space path loss	154.8		dB	Section 3.2.5	Free space path loss	145.3		dB	Section 3.2.5
Ionospheric scintillation	5.5		dB	Section 3.2.5	Ionospheric scintillation	12		dB	Section 3.2.5
Polar cap absorption	0.2		dB	Section 3.2.5	Polar cap absorption	5		dB	Section 3.2.5
Atmospheric gas attenuation	0.5		dB	Section 3.2.5	Atmospheric gas attenuation	0.5		dB	Section 3.2.5
Antenna alignment loss	0.2		dB	Section 3.2.5	Antenna alignment loss	0.2		dB	Section 3.2.5
Polarisation loss	3		dB	Section 3.2.5	Polarisation loss	3		dB	Section 3.2.5
Tracking antenna loss	3		dB	Section 3.2.5	Tracking antenna loss	2		dB	Section 3.2.5
Propagation loss		167.2	dB		Propagation loss		168.0	dB	
Receiver					**Receiver**				
Antenna gain	1.5		dBi	Dipole [52] with implementation loss	Antenna gain	1.5		dBi	Dipole [52] with implementation loss
Cable loss	1		dB	Estimate	Cable loss	0.5		dB	Estimate
BER	10^{-3}				BER	10^{-3}			
Sensitivity 2-GMSK	-118		dBm	Data from similar mission [21]	Owl VHF sensitivity 2-GMSK	-117		dBm	Green curve in [93]
Link margin		11.3	dB		Link margin		11.9	dB	

Table 3.6.: VHF and UHF downlink link budgets.

Downlink 437.305 MHz	**Data**	**Result**	**Unit**	**Source**	**Downlink 145.980 MHz**	**Data**	**Result**	**Unit**	**Source**
Transmitter					**Transmitter**				
Power out	23		dBm	Estimate	Power out	23		dBm	Owl low power[91]
Cabling losses	1		dB	Estimate	Cabling losses	0.5		dB	Estimate
Antenna gain	1.5		dBi	Dipole [52] with implementation loss	Antenna gain	1.5		dBi	Dipole [52] with implementation loss
EIRP		22.5	dBm		EIRP		22	dBm	
Propagation					**Propagation**				
Orbit height	1000		km		Orbit height	1000		km	
Slant distance 10°	3000		km		Slant distance 10°	3000		km	
Free space path loss	154.8		dB	Section 3.2.5	Free space path loss	145.27		dB	Section 3.2.5
Ionospheric scintillation	5.5		dB	Section 3.2.5	Ionospheric scintillation	12		dB	Section 3.2.5
Polar cap absorption	0.2		dB	Section 3.2.5	Polar cap absorption	5		dB	Section 3.2.5
Atmospheric gas attenuation	0.5		dB	Section 3.2.5	Atmospheric gas attenuation	0.5		dB	Section 3.2.5
Antenna alignment loss	0.2		dB	Section 3.2.5	Antenna alignment loss	0.2		dB	Section 3.2.5
Polarisation loss	3		dB	Section 3.2.5	Polarisation loss	3		dB	Section 3.2.5
Tracking antenna loss	3		dB	Section 3.2.5	Tracking antenna loss	2		dB	Section 3.2.5
Propagation loss		167.2	dB		Propagation loss		167.9	dB	
Receiver					**Receiver**				
Antenna gain	16		dBi	[46]	Antenna gain	13.1		dBi	[45]
Antenna temperature	290		K	Mostly ambient Earth temperature at 10°	Antenna temperature	290		K	Mostly ambient Earth temperature at 10°
Antenna jumper loss	2		dB	Table 3.4 with connector loss	Antenna jumper loss	1.5		dB	Table 3.4 with connector loss
Power divider loss	0.7		dB	Table 3.2	Power divider loss	0.1		dB	Table 3.2
LNA noise figure	1.25		dB	Table 3.1	LNA noise figure	1.9		dB	Table 3.1
LNA gain	22.13		dB	Table 3.1	LNA gain	23.08		dB	Table 3.1
Feedline loss	2		dB	Table 3.4 with connector loss	Feedline loss	1.5		dB	Table 3.4 with connector loss
Power amplifier insertion loss	0.1		dB	Estimate from Table 3.1	Power amplifier insertion loss	0.1		dB	Estimate from Table 3.1
WBX-40 Noise figure	3.2			[32]	WBX-40 Noise figure	5			[32]
Equivalent noise temperature	438.0		K		Equivalent noise temperature	366.6		K	
System noise temperature		728.0	K		System noise temperature		656.6	K	
System G/T		-12.6	dB/K		System G/T		-15.1	dB/K	
Signal					**Signal**				
Boltzmanns constant	-228.6		dB/K/Hz		Boltzmanns constant	-228.6		dB/K/Hz	
P_r/N_0		41.3	dB/Hz		P_r/N_0		37.6	dB/Hz	
Bandwidth	2.00E+04		Hz	[83]	Bandwidth	1.25E+04		Hz	[91] and [82]
E_b/N_0		-7.2	dB		E_b/N_0		-15.4	dB	
BER	10^{-3}				BER	10^{-3}			
Required E_b/N_0	8.4		dB	Static BER from Figure 13 in [80]	Required E_b/N_0	8.4		dB	Static BER from Figure 13 in [80]
Link Margin		-10.1	dB		Link Margin		-11.8	dB	

Discussion

For the budgeted level and elevation angle the downlink margin of -10.1 dB and -11.8 dB indicate that the links will experience frequent outages once scintillations occur. Both uplinks work with good margins of 11.3 and 11.9 dB. Figure 3.21 illustrates this by plotting the budgeted limit vs. how FSPL varies over a pass for different pass heights.

Scintillations are a sporadic phenomena, as shown by Aarons [94] and Basu [71]. Averaged occurrence is about 1%, so the proposed link budget will work in 99% of all cases. During scintillation occurrences, the ground station can support 144 MHz satellites with 400 km orbit height and 30° elevation angle for 99% of fading cases. In the 432 MHz band, satellites with 500 km orbit height and 30° elevation, are supportable. For lower fading percentiles, orbits up to 1000 km and 10° elevation are supportable. The results from the SatNOGS node also indicate that these numbers are solid.

Figure 3.21 is somewhat inaccurate due to multiple simplifications. It does not take into account that the antenna temperature gets lower as the antenna sees more of the sky. The ambient sky temperature, between 4 K and 30 K, is much lower than the ambient earth temperature, which is between 290 K and 330 K.

According to ITU [70], it is preferable to use the Global Ionospheric Scintillation Model [95] to calculate scintillation parameters. In our calculations, a static model is used, adding some inaccuracy.

There are some factors that are not included in the link budget, these are equipment degradation and coding gain. Equipment degradation is not addressed due to lack of available figures. Coding gain is not assessed as the general communication scheme for NUTS is not finished. Coding schemes could contribute with gains from approximately 2 dB to 10 dB [81].

Another factor that may be wrong in the link budget is the pointing loss. If the satellite does not point itself towards the ground station, but rather towards the center of the earth, the pointing loss will become about 3 dB higher. These factors must be updated once the capabilities of the attitude determination and control system are known.

The recorded data from the Gløshaugen SatNOGS node described in section 2.2, which contains over 200 VHF/UHF satellite passes [29], indicate that this link budget is reasonable.

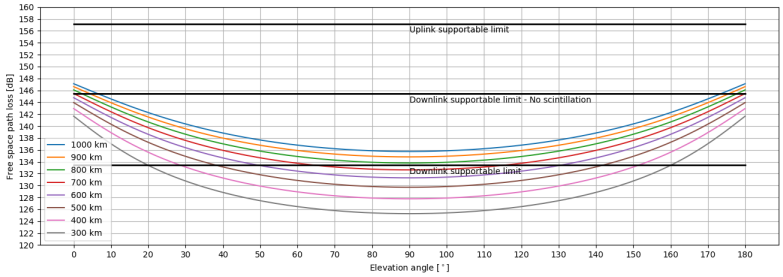

(a) Supportable VHF links.

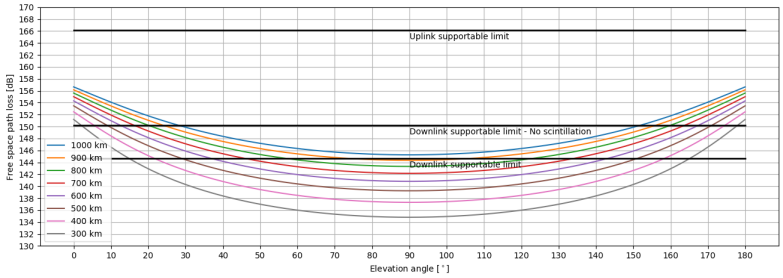

(b) Supportable UHF links.

Figure 3.21.: Path loss in relation to link budget margins for different orbit heights and elevation angles.

4. Feasibility study for low cost ultra-wideband ground station

The ground station for VHF/UHF discussed in the previous sections is designed with the band limitations of the amateur radio bands. These 20 kHz of bandwidth limit the datarate a ground station is able to supply to/from a satellite. To increase this datarate NTNU must employ higher frequencies, either in commercial or amateur radio bands.

In systems such as SatNOGS the coverage of GHz range ground stations is low. AMOS-Sat is one of the projects that would benefit from such stations. To address this, there is a need for good guidelines on how to set up such a node. There is also a need for more open-source equipment, to lower cost of adoption.

In this chapter the preliminary design of an Ultra Wideband (UWB) ground station is presented at system level. The design came to be as a mix between AMOS-Sats need for a GHz range ground station and the desire to cover additional amateur radio bands at the local amateur radio group (ARK). Combining the two gives a unique opportunity for NTNU to test components for a future ground station with low commitment.

The end goal is to give a guideline to set up a distributed network node that accommodates various implementations. A dual channel SDR is used as the central transceiver, allowing for a wide range of applications to be programmed on the fly. By using two channels and two receive/transmit chains, different polarisation schemes can be adapted dynamically, allowing operation of a large range of satellites.

The effects of polarisation diversity in a satellite communications channel are to the author's knowledge not well reported in literature. This is therefore an interesting research field. One reason that it is not frequently studied may be that satellite operations often go with established solutions, due to high project risks. Upcoming satellites with SDR payloads, such as OPS-SAT[96] and future AMOS-Sat, may allow for research in this area.

By utilising an adaptive polarisation scheme it may be possible to realise polarisation diversity. Vaughan [97] demonstrates polarisation diversity in land mobile channels and explains that it enables mitigation of certain multipath and fading phenomena. As explained by Giuli [98], polarisation diversity is commonly utilised in radar

systems to reduce false ecohes from rain, for communications this implies that altering the polarisation can reduce fading caused by rain.

Using two receive/transmit chains would traditionally imply an extreme increase in cost. Here we propose that this may actually reduce costs for certain projects. Most SatNOGS nodes are receive only. By increasing the number of LNAs to two and doing some software development, the station will be able to support LHCP, RHCP, and various linear and elliptical polarisations. For a station operator that wants to support multiple satellites, this reduces costs compared to building two separate ground stations for these services.

The ground station for AMOS-Sat should support different satellites that may employ different uplink bands. The project also has high pacing, with one satellite launch per year. If a ground station can be made to require minimal changes to support each satellite, this a major advantage. This way the development team can focus on the satellites without having to completely redesign the ground station every year.

First a literature study into available UWB technologies is conducted. Then the proposed adaptive polarisation scheme is verified. Following this, work on a prototype for ARK is presented. Finally, a specification for an AMOS-Sat ground station is presented.

4.1. Literature study on UWB ground station components

Components for a future UWB university ground station are studied and presented in this section. The scope for the survey is a ground station that is built on adaptive polarisation using SDR. The target coverage frequency is 1 GHz to 10 GHz. Total costs should be kept below 30 kEUR. The SDR used for estimations is a USRP B210 [36], that is a relatively cheap (1.2 kEUR) dual channel SDR covering 70 MHz to 6 GHz.

4.1.1. Antenna

As we saw in section 3.3.6 the free space path loss increases with frequency. To close the link budget for GHz range satellites more margin must be provided in either antenna or transmitter. The system is likely to be limited by the downlink output power, so the ground station antenna must provide enough gain to compensate.

A very common method for high gain at these frequencies is the parabolic reflector

[52]. A possible solution for the reflector is to buy kits intended for the amateur radio market. For instance, a 3 m dish kit is available for around 1.6 kEUR [99]. This dish has the specifications shown in table 4.1.

For tracking satellites, the parabolic antenna must be steerable, hence a rotor is needed. The rotor must have a resolution that is higher than the narrowest beamwidth, which usually occurs at the highest frequency. The dish kit manufacturer above stocks a rotor with 0.1° resolution for 2 kEUR.

Table 4.1.: Gain and beamwidth for a 3 m parabolic dish reflector in the amateur radio bands between 1 GHz and 11 GHz. *: Calculated from antenna size assuming perfect illumination

Frequency [MHz]	**Gain [dBi]**	**3 dB beamwidth [°]**
1296	32.4	5.7
2320	37.5	3.2
3456	40.9	2.1
5760	45.4	1.3
10368	48.1*	0.7*

Before the choice of dish is made, the required focal ratio for the feed antenna must be considered. For a feed with 100° to 150° beamwidth a centre fed dish with 0.35 to 0.5 focal ratio should be sufficient. If the beamwidth is smaller than 70°, a secondary reflector of the Cassegrain or Gregorian type may be necessary. [52]

Dual polarised feed antenna

To utilise the adaptive polarisation technique a dual linear or dual circularly polarised antenna is required. By combining the polarisation sets it is possible to synthesise a range of linear, elliptical and circular polarisations. [52]

Decade bandwidth dual polarised feed antennas is an active research field. Large radio astronomy projects like Square Kilometre Array (SKA) [100] and Very-long-baseline interferometry (VLBI) [101] are driving the technology forward.

Akgiray [102] mentions some important attributes for a dish feed. The phase center is the apparent center of radiation for an antenna [52]. It decides where the antenna should be placed in relation to the dish. If the phase center shifts with frequency the main lobe of the antenna system will also change with frequency. In order to utilise the parabolic reflector, the feed antenna must exhibit a stable pattern over the usable frequency range. If the feed pattern, particularly the 10 dB angle, changes over the frequency span, the aperture efficiency suffers. Lower aperture efficiency means that the parabolic reflector is not properly illuminated, so gain suffers. Additionally, if the 10 dB angle becomes too wide, the feed will spill over the edges of the parabolic reflector. This causes an increase in antenna temperature and

noise susceptibility. Finally the antenna pattern must be rotationally symmetric to ensure even illumination.

One of the designs that fulfils these requirements, is the eleven feed as described by Yin [103]. The eleven feed has a realisable bandwidth that is over 10:1, however the match and feed structure are very complex. A bandwidth of 10:1 means that the maximum supportable frequency is 10 times as high as the lowest frequency. This complex structure limits power handling, which is in the range of 10 W. Additionally, the complex structure causes the antenna system to become very expensive. Commercial alternatives are available on the order of 14 k EUR.

Another is the Quad Ridged Flared Horn (QRFH), some example designs are presented by Akgiray [102]. The design offers simple matching, that allows high power handling between 50 W to 100 W. The realisable bandwidth is about 6:1. Somewhat similar to the QRFH, Schwarzbeck sells a dual polarised open boundary horn [104] that has constant beamwidth from 2 GHz to 10 GHz for 5 k EUR.

Aghdam [105] presents a dual polarised sinusoidal spiral that covers 1 GHz to 5 GHz. Since the sinusoidal is a logarithmic antenna, the frequency coverage is not limited by the actual antenna structure, but rather the realisable bandwidth of the balun. Similarly to the eleven feed, the matching is complex and limits power handling to about 10 W.

4.1.2. Power amplifier

The cases where UWB transmit coverage is strictly needed are limited. However, adaptivity and frequency agility is important for a university ground station. It means that future research endeavours, such as the frequently launched AMOS satellites, can work off an existing measurement platform, cutting down on time to research. State of the art components, in particular power transistors, can be very expensive. Single band amplifiers are likely cheaper if the ground station only is required to support one satellite.

There are two amplifier architectures that allow for operation over such a large bandwidth. The first is a distributed amplifier consisting of several amplifiers that each covers a fraction of the bandwidth. These amplifiers are dynamically combined to achieve the wideband operation. The issue is that these amplifiers are very bulky, typically rack sized. The other alternative is a true wideband amplifier, where a single transistor or Monolithic Microwave Integrated Circuit (MMIC) provides the required coverage. Finally a distributed solution with two wideband amplifiers might allow for a tradeoff between coverage and physical size.

The advantage of a smaller amplifier is that it can be mounted closer to the antenna, possibly behind the feed if sufficiently miniaturised. This minimises feedline losses, which can be very significant at GHz frequencies [43][42].

Kistchinskys [106] survey of UWB gallium nitride (GaN) amplifiers from 2011 shows that emerging GaN technologies will allow for wideband operation over the frequency range that this system needs. As of 2017, two emerging solutions come close to the specification. These are the HMC8205 [107] 35 W device from Analog and the CMPA0060025F [108] 25 W device from Wolfspeed. Both devices are internally matched and cover 1 GHz to 6 GHz. The gain of both devices is about 20 dB, so a driver amplifier is needed to bring up the SDR output from 10 dBm to about 20-30 dBm in order to get the required output power. For high volumes the price for each device is approximately 500 EUR per piece. Designing with HMC8205 is easier as it features internal biasing and has slightly higher gain and output power.

Examples of suitable drivers are the CMPA0060002F [109] from Wolfspeed and HMC659LC5 [110] or HMC659LC5 [110] from Analog. The devices from Analog are internally biased. Choosing a driver and output stage from the same manufacturer is likely simpler, as they are likely to have been tested with each other.

If higher output power is required, several amplifier stages must be combined. One viable high power wideband combiner realisation is the multi-branch Wilkinson power divider [66]. An example of this divider architecture is presented by Wong [111]. Power handling in a Wilkinson divider is determined by the insertion loss and the phase mismatch between the inputs. When the inputs are mismatched, the 100 Ohm resistor sees RF power. This resistor must therefore be able to handle at least half the output power of the amplifier. Higher insertion loss results in more thermal power that the Printed Circuit Board (PCB) must handle.

Analog and Wolfspeed also provide modules that will cover 6 GHz to 18 GHz with 10 W [112] and 25 W [113] respectively. Both devices are internally matched and biased. Wilkonson combiners can be used here as well. The skin effect puts even higher demands on the thermal capabilities of the PCB as the insertion loss will be higher.

4.1.3. Low noise amplifier

Receive performance is largely determined by the noise figure of the LNA. High performance solutions use cryogenic cooling to bring down the ambient temperature of the LNA, thereby reducing the noise contribution. This is beyond the economic scope of this project, so an ambient LNA will have to be used. Commercial solutions for room temperature LNAs have noise figures as low as 0.75 dB [114] to 1.75 dB [115] dB over the range of 1 to 10 GHz.

To reduce development time, an internally matched MMIC that also integrates biasing is desirable. For these devices, vendors usually specify IP3 as the linearity measure. As touched on in section 3.2.2, IP3 is related to DR_f. Good DR_f

performance is crucial, particularly for UWB systems as the LNA must be able to handle many saturation sources in the large bandwidth. One device with NF between 1.5 and 2 dB over the 1 to 10 GHz range is the HMC753 [116] from Analog. Another device with about 1 dB more NF is the PMA2-123LN+ [117] from Minicircuits. MMA043PP4 [118] from Microsemi features similar noise figure as HMC753, but IP3 performance is considerably worse.

4.1.4. Filtering

An amplifier will generate harmonics that can cause interference for other users. This is particularly important when UWB amplifiers are coupled with UWB antennas, as harmonics within the bandwidth will radiate. Compliance standards regulate the levels of these emissions.

To address the spurious performance of the amplifier, low-pass or band-pass filtering must be applied. Filter rejection demands must be determined after measurements on the actual PA.

By adding the filters before the LNA, the number of possible interference sources can be reduced.

For high power microwave applications there are a couple of realisable filters. The filter topology that offers the lowest insertion loss and highest rejection is various cavity filter solutions [66]. Cavity filters are very narrow-band and often physically large. Another solution with slightly higher insertion loss is the stripline filter. The main advantage of the stripline in this context is that it can be made physically smaller than the cavity filter. As with the Wilkinson divider, a PCB that can handle the thermal rise due to insertion loss is necessary.

4.2. Adaptive polarisation measurement methodology

With adaptive polarisation the ground station can utilise multiple polarisations on the fly. This is useful for ground stations that are employed for many different satellite missions, especially if the requirement changes from pass to pass or even during a pass.

In order to realise adaptive polarisation, the phase difference between SDR channels must be controllable and stable for both receive and transmit.

Theoretically this is sound, as a set of identical mixers that use the same local oscillator will add the same phase to each channel [66]. This means that phase difference accuracy is likely dependent on the digital to analog conversion that

SDRs use to create baseband signals.

To verify that this is realisable, measurements using an USRP B210 [36] SDR are undertaken in this section.

4.2.1. Oscilloscope measurement

A measurement setup is devised using a R&S RTM2000 oscilloscope [119] to measure the phase difference between two outputs of a USRP B210. The setup can be seen in figure 4.2. The phase is swept in software using the gnuradio flowgraph in figure 4.1. The USRP is initially set to generate two 100 MHz carriers, due to an issue with harmonics this is later changed to 400 MHz.

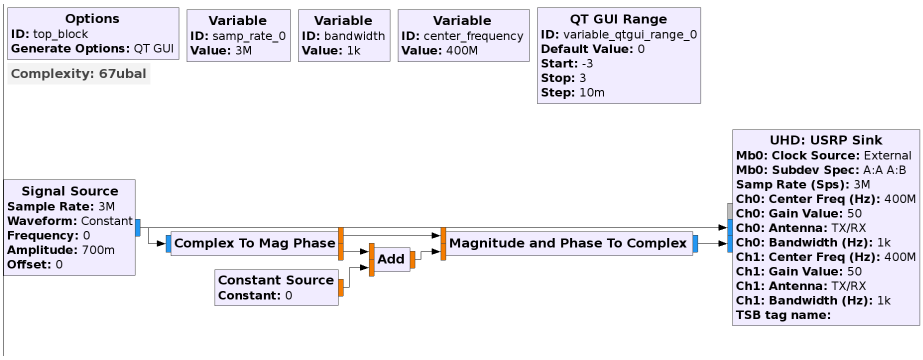

Figure 4.1.: Gnuradio schematic for adding a phase delay to one transmit port. The other port stays constant. Note: phase constant says 0, but is user configurable from -360°to 360°.

For accurate measurements the oscilloscope must have internal 50 ohm termination. Otherwise reflections from the input port will severely interfere with the measurement.

To visualise phasing combinations the oscilloscope is set in XY-mode, as shown in figure 4.3. In XY-mode, signals on one channel contribute to the X axis, while signals in the other contributes to the Y axis.

4.2.2. Signal generator measurement

To show that adaptive polarisation is realisable for receive applications, another method is needed. This time the USRP B210 will act as an oscilloscope for two signals produced from a Siglent SDG2122X [120] function generator. Channel A and B of the function generator are set to generate 100 MHz 1 V sinus signals.

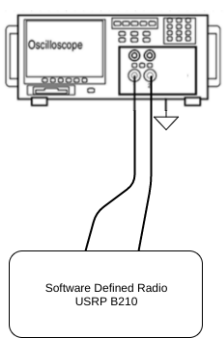

Figure 4.2.: Oscilloscope measurement of phase and amplitude differences between USRP B210 ports.

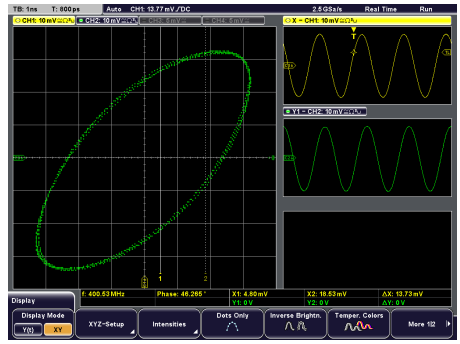

Figure 4.3.: Elliptical shape seen when combining two equal power sinusoids with 45° phase offset in oscilloscope XY-mode.

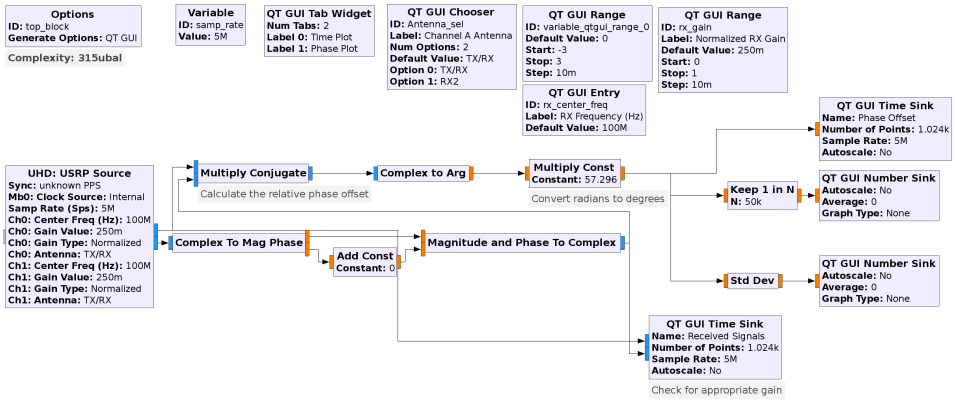

Figure 4.4.: Gnuradio block schematic for adding a phase delay to received signal. Note: phase constant says 0, but is user configurable from -180°to 180°.

Channel B is offset 90° relative to channel A. To correct for any additional offset, the phase difference is measured on a Rohde & Schwarz RTB2004 [121] oscilloscope.

For this measurement, the gnuradio flowgraph in figure 4.4 is used. The phase difference is found by performing conjugate multiplication.

4.3. Adaptive polarisation measurement results

In this section the results from the oscilloscope and signal generator measurements are presented.

4.3.1. Oscilloscope Measurement

At first glance the observed waveform is very unlike the expected sinusoidal waveform, the resulting sawtooth-like shape is seen in figure 4.5. The Fast-Fourier Transform (FFT) in figure 4.7 shows very strong harmonics, with odd harmonics as high as -10 dB below the carrier.

Figure 4.5.: 100 MHz waveform as observed by the oscilloscope.

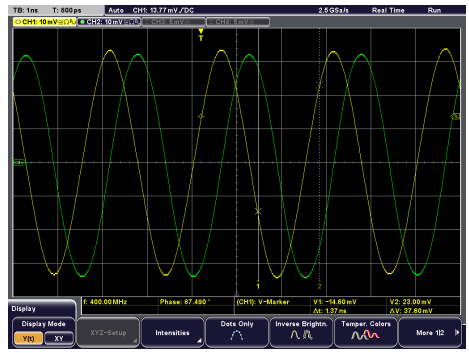

Figure 4.6.: 400 MHz waveform as observed by the oscilloscope.

To alleviate spurious problems, the scope is bandlimited to 400 MHz and the carrier frequency changed to 400 MHz. Bandlimiting the scope effectively adds a low pass filter with a cutoff frequency of 400 MHz. This technique causes harmonics to appear beyond the range of the scope. 2nd and 3rd harmonics appear at 800 MHz and 1200 MHz where they should be sufficiently attenuated. The result is the much cleaner sinusoidal waveform in figure 4.6. Figure 4.8 shows reduced third harmonic levels.

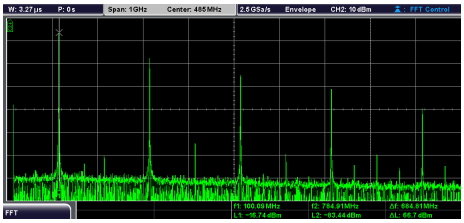

Figure 4.7.: FFT of 100 MHz, high level on odd harmonics.

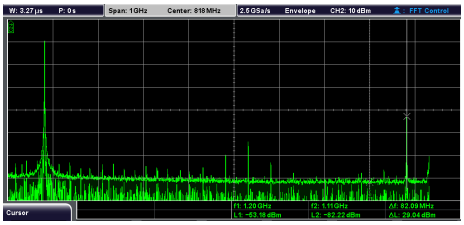

Figure 4.8.: FFT of 400 MHz, harmonic levels reduced to manageable level.

The XY-mode phase results are summarised in figure 4.9, showing that a phase difference of 90 and -90 results in a circle. Additionally, four different linear polarisations can be synthesised, as well as a range of ellipsoids.

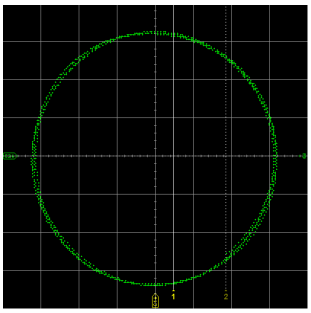

(a) Phase difference of - 90°

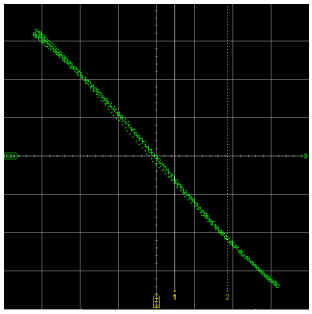

(b) Phase difference of -180°

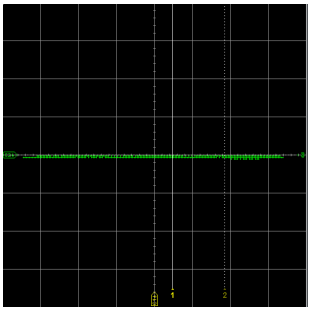

(c) Only channel 1

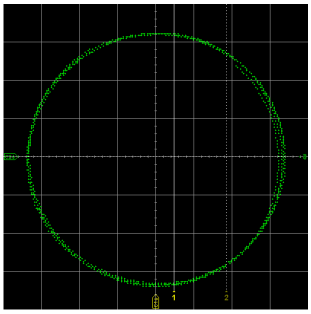

(d) Phase difference of 90°

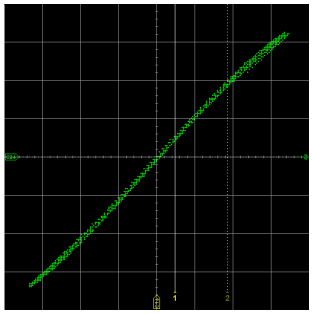

(e) Phase difference of 0°

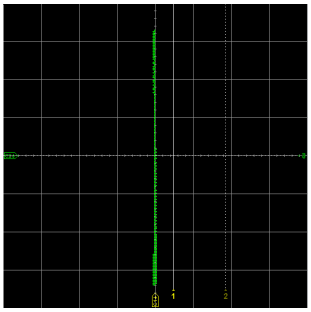

(f) Only channel 2

Figure 4.9.: A selection of phase combinations from XY-measurements on two 400 MHz carriers from a dual channel USRP B210.

The phase difference accuracy was not recorded, as oscilloscope triggering artefacts caused a phase fluctuation of +/- 2-4°. It would seem that the actual phase resolution is higher than this, but with the current measurement setup it is not observable.

4.3.2. Signal generator measurement

The oscilloscope measurement shows that adaptive polarisation is viable for transmit, next it must be shown that the phase difference is adjustable for receive applications. Results are seen in figure 4.10. The measured initial phase difference is 110°, the measurement in 4.10a shows that this also is the case for the USRP phase difference. The phase is found to be accurately adjustable. Some triggering artefacts occur, but less prominently than in the oscilloscope measurement. The phase accuracy is adjustable with at least 1° resolution.

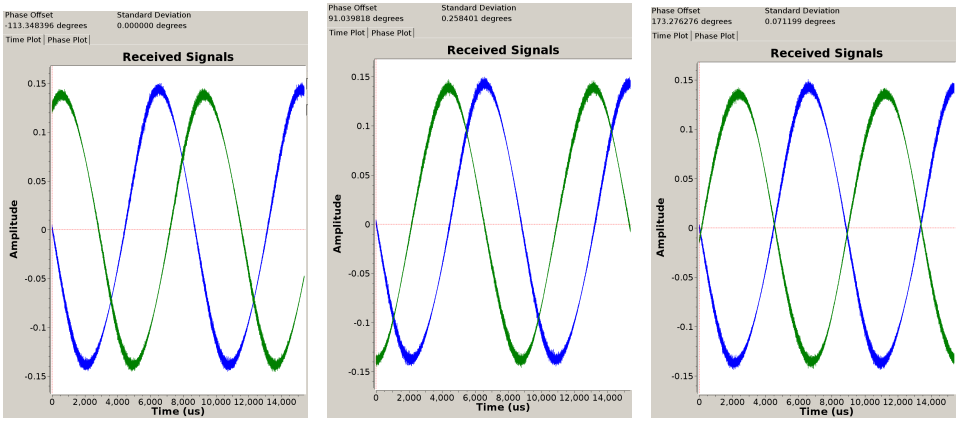

(a) Phase difference of -110°, no correction applied

(b) Phase difference of 90°, 200° correction applied

(c) Phase difference of 180°, 290° correction applied

Figure 4.10.: A selection of phase combinations created by digitally shifting the received phase using a USRP B210.

4.3.3. Discussion

The oscilloscope and signal generator measurements indicate that adaptive polarisation is viable using the USRP B210. Some issues must be investigated, however.

Harmonics generated from the USRP are problematic, particularly in a wideband system. Adding a low-pass filter as was done for the oscilloscope measurement, would limit the realisable bandwidth. One solution is to create a preselector, which is a band-pass/low-pass filterbank that is dynamically selected depending on the RF band. To address this newer generations of USRPs, such as the USRP E310 [122], feature built-in preselectors.

In a real application the phase variation with temperature and frequency must be known. Additionally it is helpful to have an indication of how the received phase

differences map to transmitted phase differences. These topics are natural parts of research into the utilisation of adaptive polarisation for link improvement.

4.4. ARK prototype

The author is involved with a project to cover 1 GHz to 10 GHz at the local amateur radio club. As suggested earlier, this provides an opportunity for NTNU to evaluate some components prior to committing resources. A brief summary of this project is presented here.

Work is started on a ground station for use in the amateur radio bands from 1 GHz to 10 GHz. A 3 m mesh parabolic reflector [99] with gain and opening angles shown in table 4.1 will be used. The focal ratio of this dish is 0.4 to 0.45. The dish is fed by a FPF R2313963 [123], which is a linear 5 band ring feed. S-parameter and antenna pattern measurements of the feed is found in appendix D. The antenna is steerable by use of a SPID Big-RAS/HR [124] rotor.

Coaxial relays are used to route between a USRP B210 SDR, amplifiers and antenna. A block diagram of the prototype is shown in figure 4.11.

The amplifiers are commercial units that each cover a single amateur radio band. The LNA is intended to be a custom build using the HMC753 [116].

The design will be highly integrated with most amplifiers and equipment being housed either behind the feedhorn or behind the dish. By doing this, cable losses are reduced significantly.

4.4.1. Software

The ground station will be hosted on a dedicated computer and controlled over internet. For the first iteration, the software will run SatNOGS. In order to access all bands in the station, an interface card must be developed to control coaxial relays and power routing. This interface card should be controlled by the computer, for example over RS232.

Tracking

As discussed in section 3.2.5 TLE inaccuracies can lead to tracking losses. With a much more directive antenna, such as the 3 m parabolic reflector used here, it is apparent that tracking losses become much more serious. Improvements in the

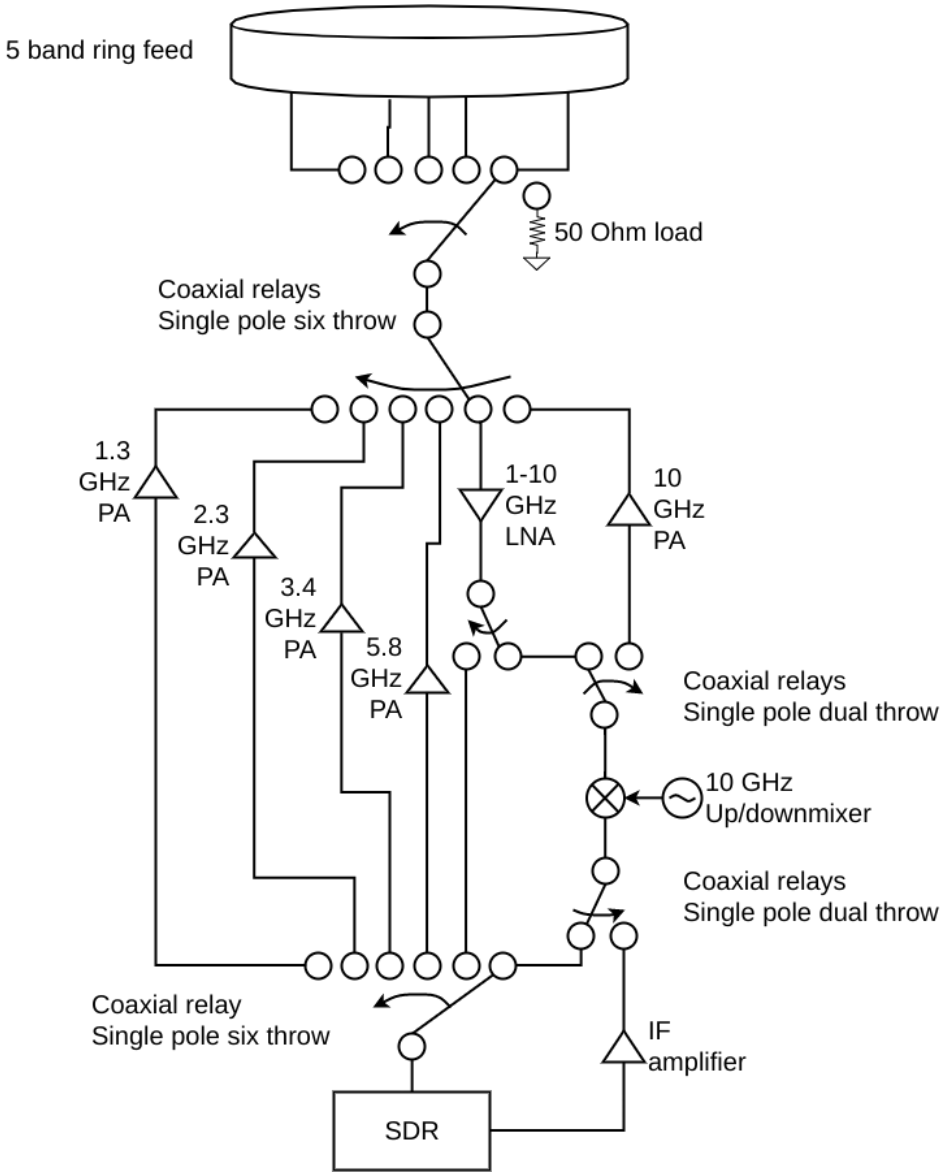

Figure 4.11.: Schematic of switches, amplifiers, mixer and filters for ARK prototype amateur radio ground station.

tracking algorithm must be considered in order to get a working system.

Hawkins [125] describes several common methods to maximise Received Signal Strength Indication (RSSI) for tracking GHz range systems. These are manual/programme

tracking, monopulse, sequential amplitude sensing and electronic beam squinting. In most systems a combination of these techniques are used, e.g. programme tracking for a rough estimate and then monopulse for fine tuning.

A high performance high complexity system might use secondary feed antennas for tracking. The system described here aims for low complexity, so monopulse and electronic beam squinting are not viable options. Sequential amplitude sensing will also have limited degrees of freedom. The available axis of motion is steering the entire antenna system in azimuth or elevation.

One way to implement this is by launching a virtual rotor controller that receives positional information from an external tracking program, e.g. SatNOGS. The accuracy of the input position can then be refined using RSSI output from gnuradio. This way the system is compatible with common software, and expandable with potential improvements that are needed to track at GHz range frequencies.

4.4.2. Thermal management

Housing the RF chain behind the feed horn has a number of advantages, but it comes with a considerable challenge in thermal management. Since the box is housed outside it needs to be waterproof, this means that heat will also be contained inside. By using a liquid cooling system a radiator may be placed outside the feed structure, for example behind the dish where it can also serve as counterweight. Care must be taken so that the system does not cause condensation or freeze during winter. Another possibility is mounting cold plates flush to the waterproof box edges and use water-rated fans on radiators mounted on the outside of the box.

The second thermal issue is sleet snow and ice accumulating on the parabolic reflector. Ice and snow can cover the holes in the mesh reflector, which will increase the windload. During winter storms this increase in wind area can have severe consequences. To amend this heating must be applied to the dish. A simple solution is zip-tying gutter heating cable to the mesh. The nominal temperature of these cables is about 5 °C. The temperature rise will deteriorate performance somewhat during winter time due to increased antenna temperature. This is a fair trade-off for longer system life.

4.5. AMOS-Sat system specification

The ground station for AMOS-Sat must be rapidly re-configurable and support many possible satellite architectures with minimal modifications. A solution that builds on the ARK prototype is presented to realise this.

The USRP B210 covers frequencies up to 6 GHz. To cover more an external mixer and synthesizer would be needed. Furthermore, the frequencies up to 6 GHz are the ones being targeted for AMOS-Sat[1]. For these reasons the system is specified to work between 1 GHz and 6 GHz.

High datarate uplink is necessary to support reprogramming the SDR that is scheduled to fly on one or more of the AMOS satellites. To this end, the ground station should feature a high power amplifier that will deliver 10-100 W output power, depending on the dish size and orbit parameters. To support all cases, a wideband amplifier covering the band between 1 GHz and 6 GHz with 100 W is specified. To simplify the design, the amplifier should be based on the HMC8205 [107]. Spurious emissions are handled by filters that are switched in by coaxial relays. The filter is the only application specific component, and for common satellite frequencies these are available commercially.

If the tests at ARK are successful, the station can employ the same 3m dish kit with rotor. With coverage between 1 GHz and 6 GHz the QRFH antenna is a reasonable low cost alternative that will handle 100 W. It can be manufactured using the process described by Akgiray [102]. The 10 dB angle may be adjusted with a change in design parameters, and the 110°beamwidth that is needed for the 3m dish is realisable. Another advantage of the QRFH design is that it may be scaled if different frequency coverage is needed in the future.

If the LNA from ARK is adequate, it can be employed at low cost. If higher performance is required, there are numerous commercial alternatives [115][114].

The example schematic is shown in figure 4.12. Mechanical coaxial switches are employed to switch between different transmit and receive configurations. To provide full output power when only one linear polarisation is needed, another Wilkinson combiner can be switched in between the amplifiers.

Approximate costs for the system is presented in table 4.2. The largest portion of the project cost will be manufacturing and design costs. One of the primary goals is to reduce the cost for later adopters by making all components available open source. The high costs will incur if multiple iterations are needed on a design or components break while prototyping. For some of the components the risk is mitigated by the ARK project. The presented solution is highly miniaturiseable so that the entire RF chain can be placed behind the feed antenna.

This specification shows that an adaptive polarisation ground station covering multiple octaves in the 1 GHz to 10 GHz range is feasible. The full decade bandwidth can also be realised, albeit at a lower power level and higher cost, using an eleven feed and distributed amplifier.

Table 4.2.: Cost estimate for 1 GHz to 6 GHz ground station

Component	**Number**	**Cost low[EUR]**	**Cost high [EUR]**	**Source**
Parabolic reflector	1	1600	1600	RF Hamdesign [99]
Rotor	1	2000	2000	RF Hamdesign [124]
USRP B210	1	1400	1400	Ettus Research [36]
LNA - HMC753	2	150	600	Analog Devices [116]
LNA - PCB costs	2	150	600	Estimate
PA - HMC8205	4	2000	6000	Analog Devices [107]
PA driver - HMC659LC5	2	600	1800	Analog Devices [126]
PA - PCB costs	1	500	1500	Estimate
QRFH manufacturing cost	1	2000	6000	Estimate
Coaxial switches	10	3000	3000	Pasternack [127]
Cooling solution	1	1000	3000	Estimate
Additional costs	1	1000	2000	Cables, mechanical work
Sum		**15400**	**29500**	

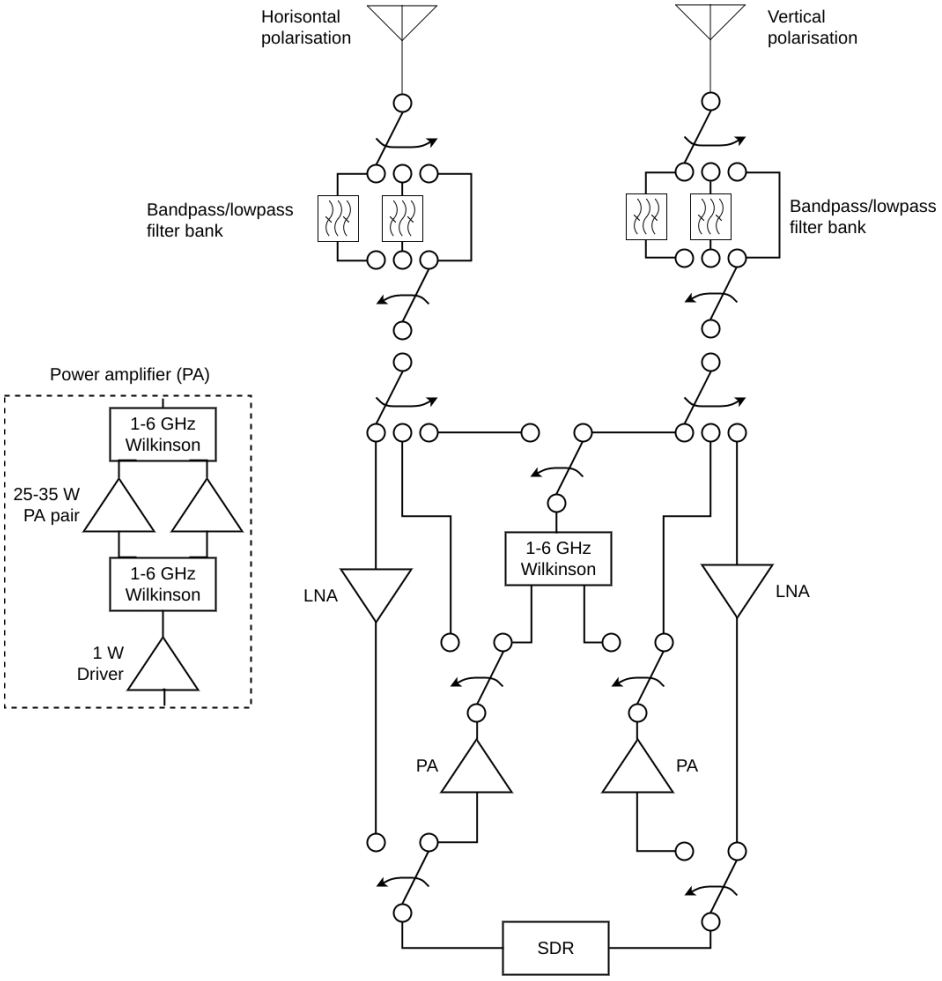

Figure 4.12.: Schematic of switches, amplifiers and filters for 1 to 6 GHz operation.

5. Conclusion and further work

NTNU AMOS is expanding with a satellite programme. In order to support these future satellites, a study into ground station design and verification was conducted.

An open ground station network is an emerging platform design that provides an open-source alternative to commercial ground station networks. A survey of such services was conducted in chapter 2.One of these services, SatNOGS [6], was further evaluated by setting up the Gløshaugen VHF/UHF ground station as a node. During the spring of 2017 this node has tracked and recorded over 200 satellite passes [29], showing that the SatNOGS framework is viable.

The verification and setup of the Gløshaugen ground station was described in section 3.2. The results show that the ground station can support 144 MHz satellites with 400 km orbit height and 30° elevation angle for 99% of fading cases. In the 432 MHz band, satellites with 500 km orbit height and 30° elevation are supportable. For lower fading percentiles orbits up to 1000 km and 10° elevation are supportable. The results from the SatNOGS node also indicate that these numbers are solid.

AMOS-Sat is planning to use sensors such as hyper spectral cameras and synthetic aperture radar. A 1 GHz to 6 GHz ground station to support these high datarate applications was shown to be realisable. The ground station supports adaptive polarisation, which is shown to be realisable on the selected SDR platform in section 4.2. Work is started on a 3 m parabolic dish that will cover the amateur radio bands between 1 GHz and 10 GHz for the local student amateur radio group (ARK). This project allows for testing some components used in the 1 GHz to 6 GHz system before committing to a ground station solution for AMOS-Sat.

A specification for a wideband system that builds on the ARK project was proposed in section 4.5. The system uses commercially available components and covers 1 GHz to 6 GHz continuously with 100 W output power. This specification shows that the design and implementation of a multi-octave single feed ground station in the 1 GHz to 10 GHz range is feasible.

The uplink amplifiers for the Gløshaugen ground station are scheduled to arrive mid July 2017. These must be tested using the verification steps in section 3.2.4. After testing they should be integrated into the ground station rack. Once the amplifiers are in place and tested the station will be ready for uplink.

SatNOGS features open-source software and hardware. To further improve the system, contributions are necessary. One example is to open-source the ground station design for AMOS-Sat.

To the author's knowledge, utilisation of polarisation diversity for satellite communications channels is not reported in literature. The ground station specified in section 4.5 is capable of doing such research, particularly when coupled with upcoming missions such as AMOS-Sat that are flying SDRs.

Commercially available ground station components will be tested on ARKs 1 GHz to 10 GHz ground station during the fall of 2017. Following these tests, NTNU must revisit its needs and plan for a GHz range ground station to support new satellite endeavours, the ideas proposed in this thesis provides a starting point. The systems described and built in this thesis, as well as access to the SatNOGS network, will fulfil NTNUs need for ground station services and enable a ground station headquarter for the AMOS satellites.

Appendices

A. Troubleshooting ground station failure

There are several components in the ground station setup that have a life expectancy that is shorter than the mission duration. In order to keep the station running, a list of components that may break, how to identify them and how to fix them, is presented here.

Rotor controller: Mechanical relays are used in the G5500 rotor controller, while tracking a satellite these are switched on and off hundreds of times. Eventually these will break. To verify that the relays are broken, the operator can try manually steering the rotor with the control box. During normal operation the clicking sound will be audible. If no click is heard, something is wrong.

The spare rotor controller, G5400B, can be put into service as a replacement. A more thorough investigation into the G5500 should be performed, possibly replacing the broken relays or other broken components.

Low noise amplifier: The LNA also uses mechanical relays to switch between transmit and receive states. Since the relays in the LNA are triggered by RF-sense they have to experience some live switching. Live switching means that the internal relays in the LNA sees some RF power while they are in the switching state. This decreases the life expectancy of the relay.

To identify if the LNA has stopped working, the current draw over the DC-injector should be checked. If the current draw differs significantly from what the datasheet specifies, something is wrong. It is also possible to listen for audible clicks when power is provided to the LNA.

If an LNA is broken, the spare LNA(s) may be installed.

Power amplifier: Similarly, the power amplifier also uses RF-sensed switching at the same duty cycle as the LNA. However, the pass-through power is much lower, so it is not as likely to break.

If it does break the ground station will not be able to uplink to the satellite. If this happens, first check the fuse on the power divider. If the fuse is not blown, try attaching an RF power meter between the power amplifier and the antenna and

see if there is any output power. If there is no output power contact TESystems for support.

Rotor: Since the rotor is situated outdoors there may be some corrosion. Likely the rotor will start failing in either Azimuth or Elevation, if both fail simultaneously the error is probably with the rotor controller. To diagnose failing azimuth/elevation rotors, start by investigating if there is any breakage in the control lines between rotor and rotor controller. If the lines seem intact, try listening if there is any motor activity when the rotation buttons are pressed. In case there is not any audible motion, try opening the rotor and see if something is jammed inside. If there is no sounds coming from the rotor, the DC motors inside may be dead. Look into finding replacements or buy a new rotor.

B. LNA NF and Gain

In this section the measured NF and gain curves of the SP-200, SP-2000, SP-70 and SP-7000 LNAs from section 3.3.2 are presented. The curves for SP-200 and SP-2000 are shown in figure B.1, and the curves for SP-70 and SP-7000 are shown in figure B.2.

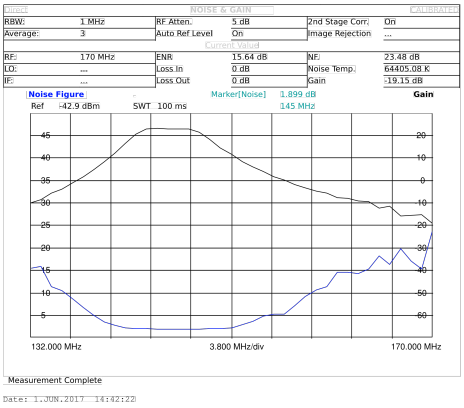

(a) SP-2000 high gain setting.

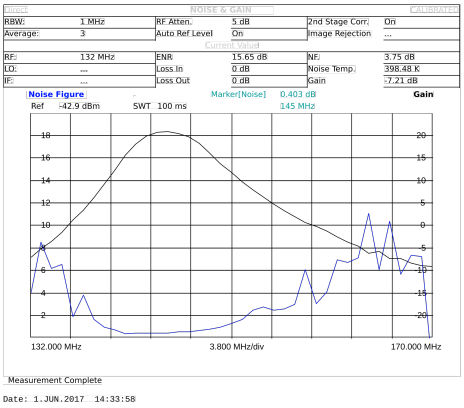

(b) SP-200 high gain setting.

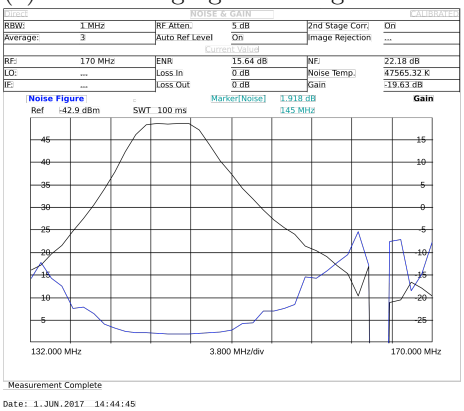

(c) SP-2000 medium gain setting.

(d) SP-200 medium gain setting.

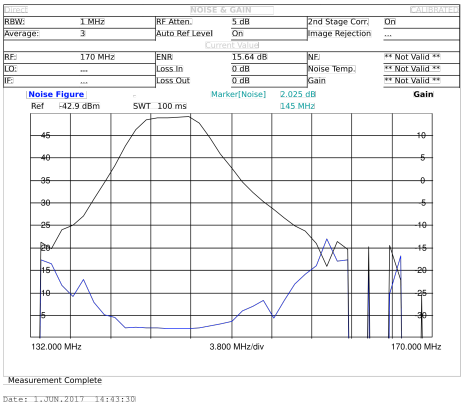

(e) SP-2000 low gain setting.

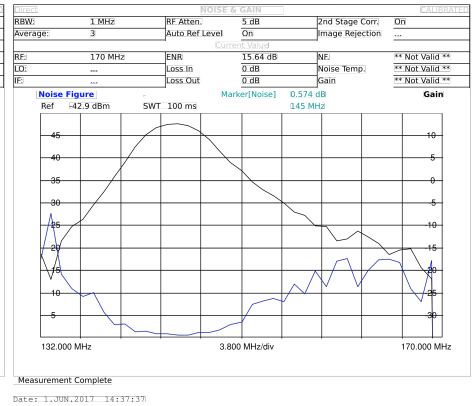

(f) SP-200 low gain setting.

Figure B.1.: Noise figure and gain measurements of SP2000 and SP200 LNAs.

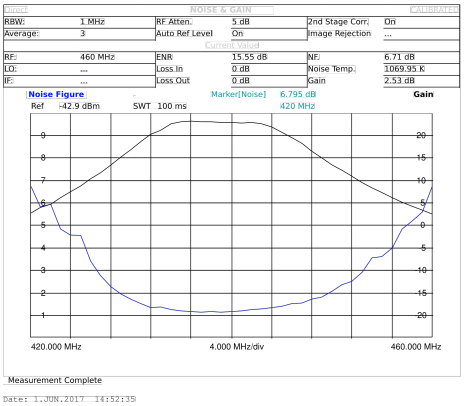

(a) SP-7000 high gain setting.

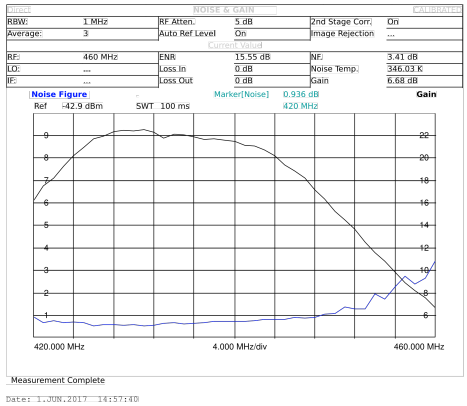

(b) SP-700 high gain setting.

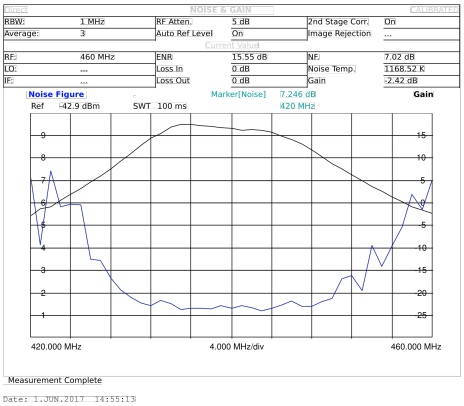

(c) SP-7000 medium gain setting.

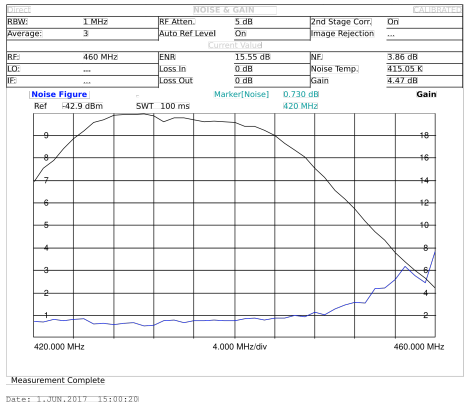

(d) SP-70 medium gain setting.

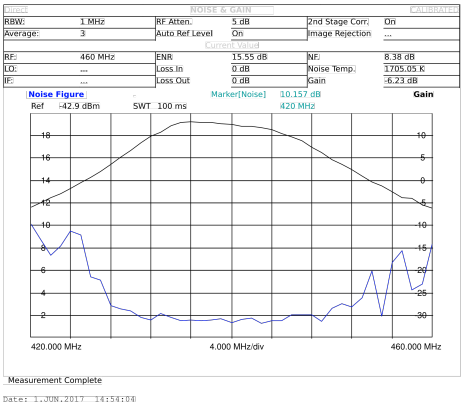

(e) SP-7000 low gain setting

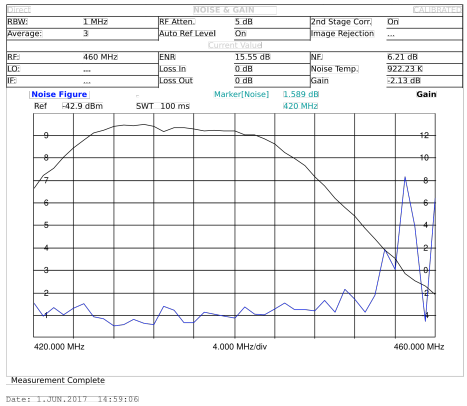

(f) SP-70 low gain setting

Figure B.2.: Noise figure and gain measurements of SP7000 and SP70 LNAs.

C. SatNOGS-client build instructions

Build instructions for setting up a SatNOGS-client installation the first time. This is valid for SatNOGS version 0.3, refer to build instructions on GitHub for future versions of SatNOGS-client [17] and GR-SatNOGS [20].

```
// Before starting, register an account on network-dev.satnogs.org and create
// a ground station there.
// Installation is based on a fresh ubuntu 17.04 desktop install
// Start by making sure the system is up to date.
sudo apt-get update
sudo apt-get upgrade

// SatNOGS uses bleeding edge versions gnuradio, following the guidelines in
// http://gqrx.dk/download/install-ubuntu get the most up to date resources.
sudo apt-get purge --auto-remove gqrx
sudo apt-get purge --auto-remove gqrx-sdr
sudo apt-get purge --auto-remove libgnuradio*

sudo add-apt-repository -y ppa:bladerf/bladerf
sudo add-apt-repository -y ppa:ettusresearch/uhd
sudo add-apt-repository -y ppa:myriadrf/drivers
sudo add-apt-repository -y ppa:myriadrf/gnuradio
sudo add-apt-repository -y ppa:gqrx/gqrx-sdr
sudo apt-get update

// If this works without errors proceed with installing gqrx
// (will pull in relevant gnuradio dependencies).
sudo apt-get install gqrx-sdr

// Next install the dependencies for gr-satnogs and satnogs-client.
sudo apt-get install git gcc python-dev vorbis-tools libhamlib-dev libhamlib-utils
cmake swig libfftw3-dev libcppunit-dev doxygen gr-osmosdr libnova-dev gnuplot
```

```
libvorbis-dev libffi-dev openssl libpng-dev python-pip libssl-dev vim redis-tools
redis-server python-gevent python-gevent-server

// Build and install gr-satnogs from source.
git clone https://github.com/satnogs/gr-satnogs.git
cd gr-satnogs/
mkdir build
cd build
cmake -DLIB_SUFFIX=64 -DCMAKE_INSTALL_PREFIX=/usr ..
make
sudo make install
sudo ldconfig
cd

// Build and install satnogs-client from source.
git clone https://github.com/satnogs/satnogs-client.git
cd satnogs-client
sudo pip install -e .
python setup.py build
sudo python setup.py install
cd

// Add the user to the dialout group (check group permissions by typing "groups" in
// terminal), this is needed for controlling rotors via serial port.
sudo useradd -aG dialout username
sudo reboot // Needed to register changes

// Start rotctld with your rotor parameters in a separate terminal window.
rotctld -m 603 -r /dev/ttyUSB0

// Create a .env file, I use vim, you can use whatever text editor you prefer.
vim ~/.env

// Fill in the following (must match your satnogs network info)
// SATNOGS_RX_DEVICE should match your receiver.
export SATNOGS_API_TOKEN="dummy_api_token_here"
export SATNOGS_STATION_ID="65"
export SATNOGS_STATION_LAT="40.662"
export SATNOGS_STATION_LON="23.337"
export SATNOGS_STATION_ELEV="150"
```

```
export SATNOGS_NETWORK_API_URL="https://network-dev.satnogs.org/api/"

export SATNOGS_RX_DEVICE="rtlsdr"

// Save and close the file, then register it by running.
source ~/.env

// Start satnogs-client.
satnogs-client

// Observations may now be scheduled from network-dev.satnogs.org.
```

D. Measurements on RFhamdesign dish feed

S11 measurements are done on an Agilent E8364B[128] network analyser using the HP 85052D[129] calibration kit. The results are seen in figure D.4. The S11 measurement for the 5760 MHz port is very high, indicating that something is broken or wrong with the measurement setup.

The antenna patterns are measured in NTNUs antenna hall using a ETS Lindgren Model 3117 horn[130]. The antenna patterns are shown in figures D.1,D.2 and D.3 the 3 dB angles are marked out in red, 10 dB angles are marked in green. The 10 dB angles are between 90° and 150°. This means that the ARK dish will likely have somewhat higher antenna temperature due to spillover at certain frequencies and poor utilisation of the parabolic reflector at other frequencies.

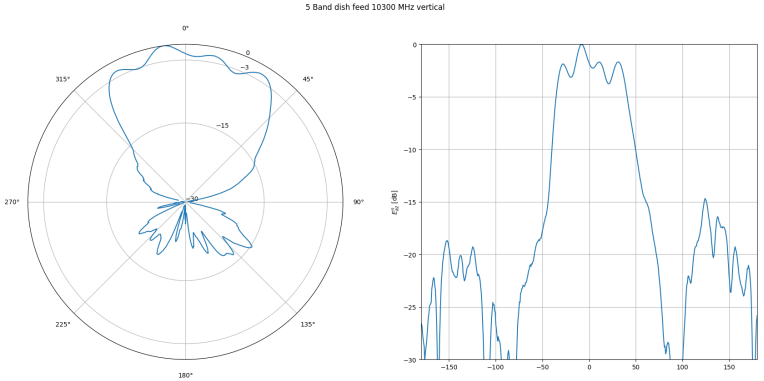

(a) 10368 MHz vertical pattern. 10 dB angle: N/A.

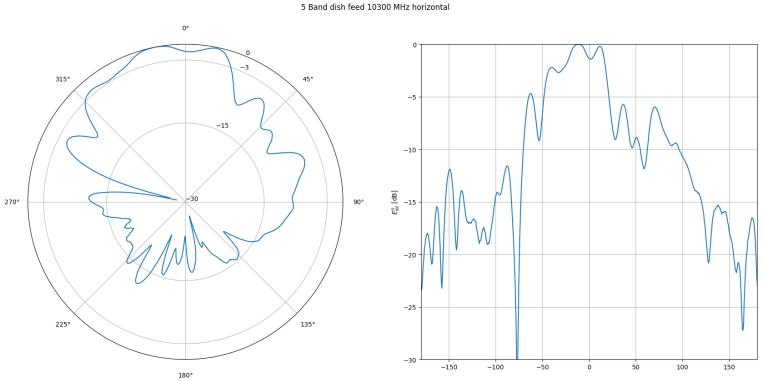

(b) 10368 MHz horizontal pattern. 10 dB angle: N/A.

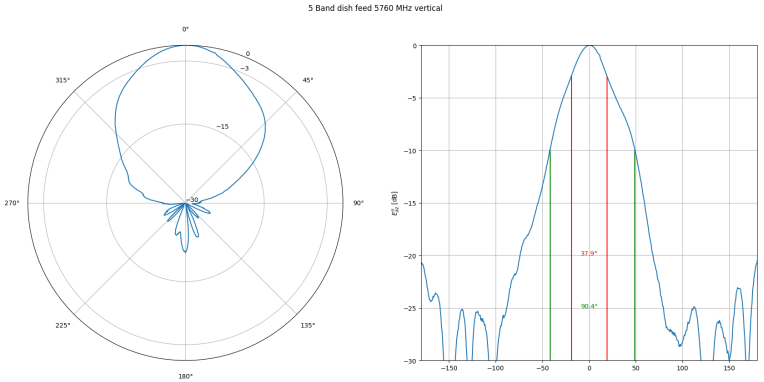

(c) 5760 MHz vertical pattern. 10 dB angle: 90.4°.

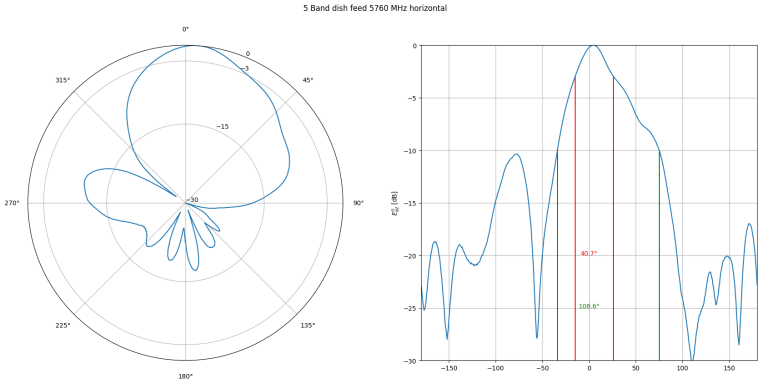

(d) 5760 MHz horizontal pattern. 10 dB angle: 108.6°.

Figure D.1.: 5 band dish feed antenna patterns.

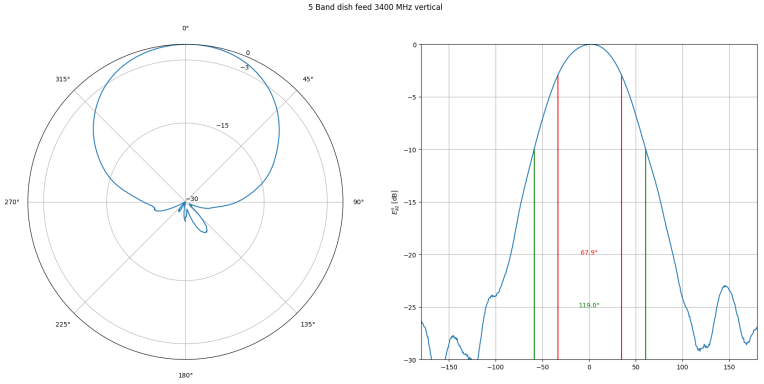

(a) 3400 MHz vertical pattern. 10 dB angle: 119.0°.

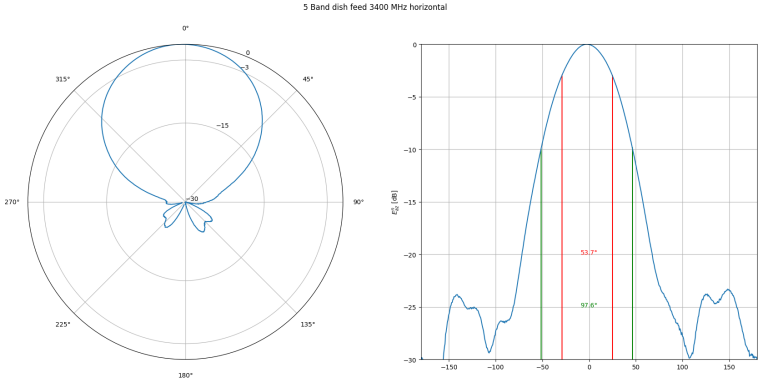

(b) 3400 MHz vertical pattern. 10 dB angle: 119.0°.

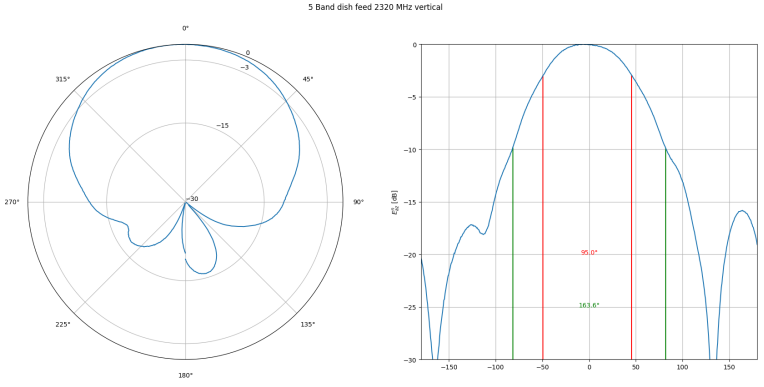

(c) 2320 MHz vertical pattern. 10 dB angle: 163.6°.

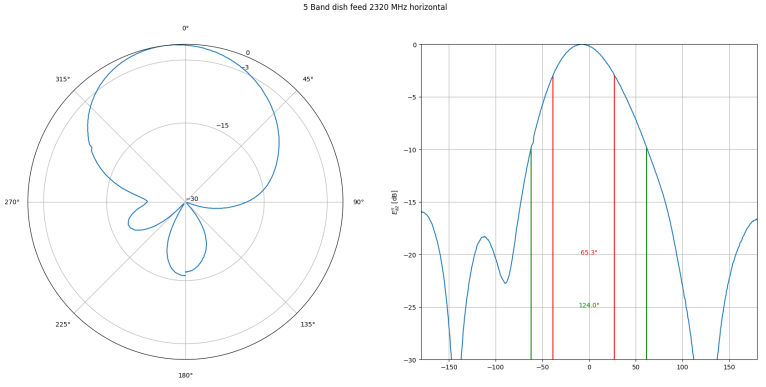

(d) 2320 MHz horizontal pattern. 10 dB angle: 124.0°.

Figure D.2.: 5 band dish feed antenna patterns.

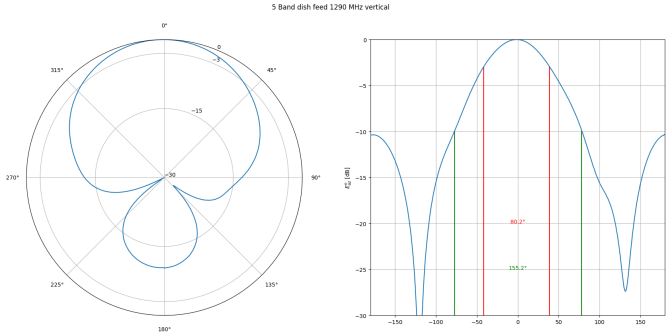

(a) 1296 MHz horizontal pattern. 10 dB angle: 155.2°.

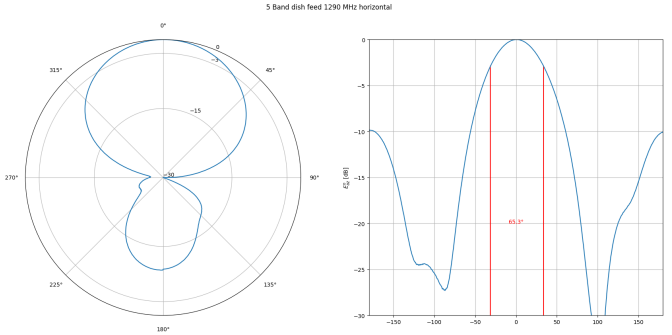

(b) 1296 MHz horizontal pattern. 10 dB angle: N/A.

Figure D.3.: 5 band dish feed antenna patterns.

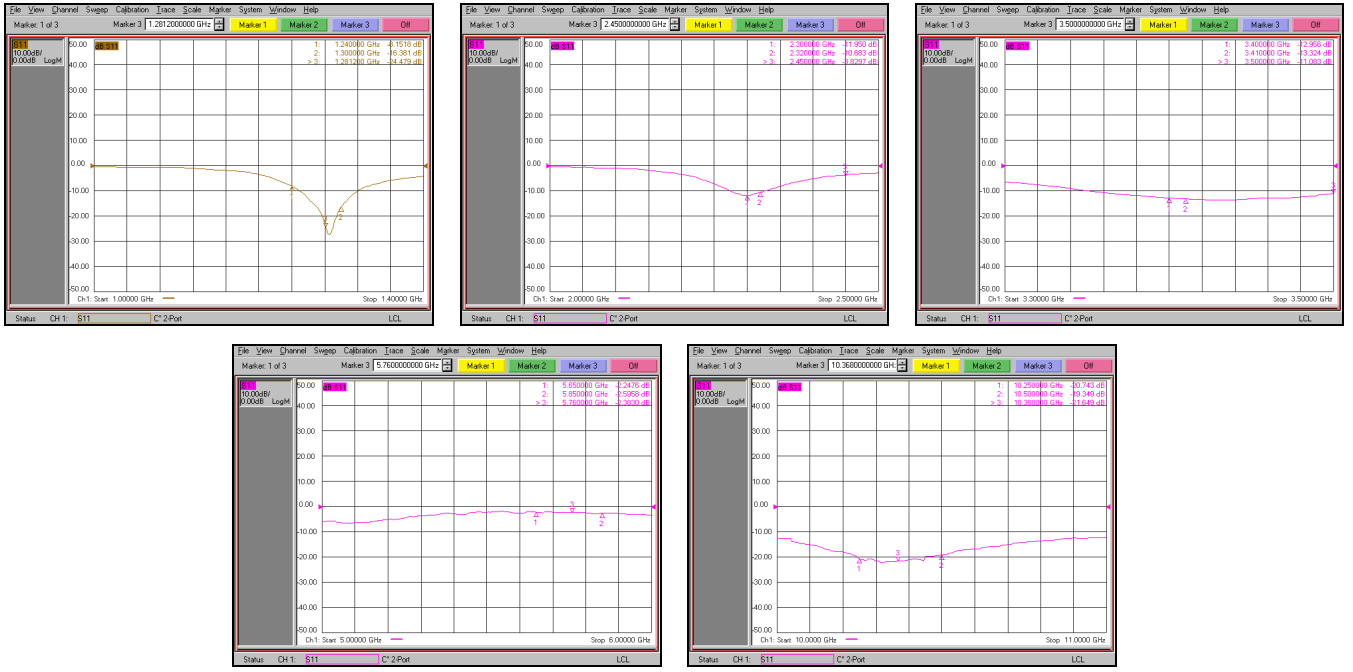

Figure D.4.: S11 measurements for 5 band dish feed

Bibliography

[1] Rajan, Kanna and Johansen, Tor Arne and Sørensen, Asgeir and Birkeland, Roger. A Roadmap for a SmallSat Program. 2016.

[2] Malcolm Macdonald and Viorel Badescu. *The international handbook of space technology*. Springer, 2014.

[3] International Telecommunication Union. M.1371-5 (02/2014) Technical characteristics for an automatic identification system using time division multiple access in the VHF maritime mobile frequency band, 2015.

[4] International Telecommunication Union. M.2092-0 (10/2015) Technical characteristics for a VHF data exchange system in the VHF maritime mobile band, 2015.

[5] Kyle Leveque, Jordi Puig-Suari, and Clark Turner. Global educational network for satellite operations (genso). 2007.

[6] Libre Space Foundation. *SatNOGS Satellite Networked Open Ground Station*. Available online at `https://satnogs.org/`, with source code at `https://github.com/satnogs`, accessed May 2017.

[7] The Distributed Ground Station Network project blog. Available online at `https://hackaday.io/project/10743-the-distributed-ground-station-network`, accessed May 2017.

[8] ThumbSat project website. Available online at `https://www.thumbsat.com/thumbnet`, accessed May 2017.

[9] Leffke, Zachary James. *Distributed ground station network for cubesat communications*. PhD thesis, Virginia Tech, 2013.

[10] Dascal, Vlad and Dolea, Paul and Cristea, Octavian and Palade, Tudor. Low-cost SDR-based ground receiving station for LEO satellite operations. In *Telecommunication in Modern Satellite, Cable and Broadcasting Services (TELSIKS), 2013 11th International Conference on*, volume 2, pages 627–630. IEEE, 2013.

[11] Bosco, Marco and Tortora, Paolo and Cinarelli, Davide. Alma Mater Ground Station transceiver: A software defined radio for satellite communications. In *Metrology for Aerospace (MetroAeroSpace), 2014 IEEE*, pages 549–554. IEEE, 2014.

[12] Forskrift om radioamatørlisens, Available online at https://lovdata.no/dokument/SF/forskrift/2009-11-05-1340, accessed May 2017.

[13] Systems Toolkit (STK) Product page. Available online at https://www.agi.com/products/engineering-tools, accessed May 2017.

[14] Libre Space Foundation. *SatNOGS Network*. Available online at https://network.satnogs.org/, accessed May 2017.

[15] Libre Space Foundation. *SatNOGS Development Network*. Available online at https://network-dev.satnogs.org/, accessed May 2017.

[16] Libre Space Foundation. *SatNOGS DB*. Available online at https://db.satnogs.org/, accessed May 2017.

[17] Libre Space Foundation. *SatNOGS Ground Station CLient Software*. Available online at https://github.com/satnogs/satnogs-client, accessed May 2017.

[18] Hamlib Website. Available online at https://sourceforge.net/p/hamlib/wiki/Hamlib/, accessed December 2016.

[19] GNU Radio Website. Available online at http://www.gnuradio.org, accessed December 2016.

[20] Libre Space Foundation. *SatNOGS GNU Radio Out-Of-Tree Module*. Available online at https://github.com/satnogs/gr-satnogs, accessed May 2017.

[21] Upsat COMMS Communications Subsystem description. Available online at https://upsat.gr/?page_id=22, accessed May 2017.

[22] Libre Space Foundation. *SatNOGS Antennas*. Available online at https://github.com/satnogs/satnogs-antennas, accessed May 2017.

[23] Libre Space Foundation. *SatNOGS Rotator project*. Available online at https://github.com/satnogs/satnogs-rotator, accessed May 2017.

[24] Libre Space Foundation. *Controller electronics and firmware for SatNOGS rotator*. Available online at https://github.com/satnogs/satnogs-rotator-controller, accessed May 2017.

[25] Dascal, Vlad and Dolea, Paul and Palade, Tudor and Cristea, Octavian. Aspects of a Low-Cost Ground Station Development for GENSO Network. *Acta Technica Napocensis*, 52(4):36, 2011.

[26] DGSN github project page. Available online at https://github.com/aerospaceresearch/DGSN_bigwhoop, accessed May 2017.

[27] Rafael Micro. *R820T High Performance Low POwer Advanced Digital TV Silicon Tuner Datasheet*. Available online at `http://rtl-sdr.com/wp-content/uploads/2013/04/R820T_datasheet-Non_R-20111130_unlocked.pdf`, accessed May 2017.

[28] Libre Space Foundation. *Installing SatNOGS on a Raspberry Pi 3*. Available online at `http://satnogs.readthedocs.io/en/stable/satnogs-client/doc/raspi-install.html`, accessed May 2017.

[29] SatNOGS development station 88 - LA1NGS. Available online at `https://network-dev.satnogs.org/stations/88/`, accessed May 2017.

[30] Karlsen, Øyvind. Prestudy on Local Radio Channel Dynamics and Diversity for VHF Satellite Communications. December 2016.

[31] Ettus Research. *USRP2*. Available online at `https://kb.ettus.com/USRP2`, accessed May 2017.

[32] Ettus Research. *WBX-40 Test report*. Available online at `http://files.ettus.com/performance_data/wbx/WBX-without-UHD-corrections.pdf`, accessed May 2017.

[33] Ettus Research. *The USRP Hardware Driver Repository*. Available online at `https://github.com/EttusResearch/uhd`, accessed May 2017.

[34] Cheng, C.-L. and Chang, F.-R. and Tu, K.-Y. Highly Accurate Real-Time GPS Carrier Phase-Disciplined Oscillator. *IEEE Transactions on Instrumentation and Measurement*, 54(2):819–824, Apr 2005.

[35] J. Miles KE5FX. *Some GPSDO Performance Comparisons*. Available online at `http://www.ke5fx.com/gpscomp.htm`, accessed December 2016.

[36] Ettus Research. *USRP Hardware Driver and USRP Manual*. Available online at `http://files.ettus.com/manual/page_usrp_b200.html`, accessed December 2016.

[37] LimeSDR product page. Available online at `https://myriadrf.org/projects/limesdr/`, accessed May 2017.

[38] TE Systems 1448RA product page, Available online at `http://www.tesystems.com/am-radio.htm`, accessed May 2017.

[39] WBX-40 Product website. Available online at `https://www.ettus.com/product/details/WBX`, accessed May 2017.

[40] West Mountain Radio. *RIGrunner for model 8012*. Available online at `http://www.westmountainradio.com/pdf/RR8012manual.pdf`, accessed May 2017.

[41] Astron Corporation product website. Available online at `http://www.astroncorp.com/showpage.asp?p=2`, accessed May 2017.

[42] Draka Cableteq. *RFA 1/2" Coaxial Cable*. Available online at http://media.draka.no/2015/06/RFA-012-5005-061.pdf, accessed December 2016.

[43] Times Microwave. *MIL-C-17 Coaxial cables*. Available online at http://disti-assets.s3.amazonaws.com/cdmelectronics/files/datasheets/4697.pdf, accessed December 2016.

[44] SSB Electronics. *SP-6/ SP-2000/ SP-220/ SP-7000 SUPER AMP GaAsFET SERIES 50,144,220 432/435 MHz. Mast-Mounted Preamplifiers*. Available online at http://gatorradio.org/Manuals/SSB_SP-7000_preamp_manual.pdf, accessed December 2016.

[45] AFT. *2x9 elements Yagi antenna*. Available online at https://www.f9ft.com/pdf/220818e.pdf, accessed December 2016.

[46] AFT. *2x19 elements crossed Yagi antenna*. Available online at https://www.f9ft.com/pdf/220938e.pdf, accessed December 2016.

[47] Yaesu MUSEN CO., LTD. *INSTRUCTION MANUAL G5500*. Available online at https://www.yaesu.com/downloadFile.cfm?FileID=8814&FileCatID=155&FileName=G-5500_IM_ENG_E12901004.pdf&FileContentType=applicationFpdf, accessed December 2016.

[48] Yaesu MUSEN CO., LTD. *YAESU GS-232A Computer Control Interface for Antenna Rotators*. Available online at https://www.yaesu.com/downloadFile.cfm?FileID=820&FileCatID=155&FileName=GS232A.pdf&FileContentType=application%2Fpdf, accessed December 2016.

[49] Klofas, Bryan and Anderson, Jason and Leveque, Kyle. A survey of cubesat communication systems. In *5th Annual CubeSat Developers' Workshop*, 2008.

[50] Klofas, Bryan and Leveque, Kyle. A survey of cubesat communication systems: 2009-2012. In *10th Annual CubeSat Developers' Workshop*, 2013.

[51] Davies, Kenneth and Smith, Ernest K. Ionospheric effects on satellite land mobile systems. *IEEE Antennas and Propagation Magazine*, 44(6):24–31, 2002.

[52] Balanis, Constantine A. *Antenna theory: analysis and design*. John Wiley & Sons, 2005.

[53] Wimo Antennen und Electronic GmbH. Power divider product page. Available online at http://www.wimo.com/power-splitter-combiner_e.html, accessed May 2017.

[54] AFT F9FT. *Notice sur la Polarisation circulaire*. Available online at http://f5ad.free.fr/QSP_Antennes/ANT-QSP_F9FT_polcircfr.pdf ,accessed May 2017.

[55] SSB Electronics. *SP 200 Pre-Amp switchable 145 MHz*. Available online at http://www.ssb.de/amplifiers/preamplifier/vox/100w/sp-200-pre-amp-switchable-145-mhz, accessed December 2016.

[56] SSB Electronics. *SP 70 Pre-Amp switchable 435 MHz*. Available online at http://www.ssb.de/amplifiers/preamplifier/vox/100w/sp-70-pre-amp-switchable-435-mhz, accessed December 2016.

[57] Rohde & Schwarz. *R&S SMU200A Signal Generator Specifications*. Available online at https://cdn.rohde-schwarz.com/pws/dl_downloads/dl_common_library/dl_brochures_and_datasheets/pdf_1/SMU_dat-sw-en.pdf, accessed May 2017.

[58] Rohde & Shwarz. *R&S FSV-K30 Noise Figure Measurements Operating Manual*. Available online at https://cdn.rohde-schwarz.com/pws/dl_downloads/dl_common_library/dl_manuals/gb_1/f/fsv_1/FSV_K30_NoiseFigure_UserManual_en_04.pdf, accessed May 2017.

[59] Aim & Thurlby Thandar Instruments. *EL-R & EX-R Series*. Available online at http://resources.aimtti.com/datasheets/psu-elr-exr-series-7p.pdf, accessed May 2017.

[60] Keysight Technologies. *Keysight 346A/B/C Noise Source (Including Options 001 and 004)*. Available online at http://literature.cdn.keysight.com/litweb/pdf/00346-90148.pdf?id=1000002290-1:epsg:man, accessed May 2017.

[61] David M David M Pozar. *Microwave and RF wireless systems*. John Wiley & Sons,, 2001.

[62] Rohde & Schwarz. *R&S SMU200A Signal Generator Specifications*. Available online at https://cdn.rohde-schwarz.com/pws/dl_downloads/dl_common_library/dl_brochures_and_datasheets/pdf_1/SMU_dat-sw-en.pdf, accessed May 2017.

[63] Sherwood Engineering receiver test table. Available online at http://www.sherweng.com/table.html, accessed May 2017.

[64] Rohde & Schwarz. *R&S ZNB Network Analyzer Specifications*. Available online at https://cdn.rohde-schwarz.com/pws/dl_downloads/dl_common_library/dl_brochures_and_datasheets/pdf_1/service_support_30/ZNB_dat-sw_en_5214-5384-22_v0900_96dp.pdf, accessed May 2017.

[65] Keysight Technologies. *Keysight Technologies 85052B 3.5 mm Calibration Kit*. Available online at http://literature.cdn.keysight.com/litweb/pdf/85052-90077.pdf?id=1000000554:epsg:man, accessed May 2017.

[66] Pozar, David M. *Microwave engineering*. John Wiley & Sons, 2009.

[67] Advanced Design System (ADS) product website. Available online at http://www.keysight.com/en/pc-1297113/advanced-design-system-ads?cc=US&lc=eng, accessed May 2017.

[68] Keysight MSO9254A Mixed Signal Oscilloscope product page. Available online at http://www.keysight.com/en/pdx-x201762-pn-MSO9254A/mixed-signal-oscilloscope-25-ghz-4-analog-plus-16-digital-channels?cc=US&lc=eng, accessed May 2017.

[69] Rohde & Shwarz. *RS FSH Handheld Spectrum Analyzer*. Available online at https://cdn.rohde-schwarz.com/pws/dl_downloads/dl_common_library/dl_brochures_and_datasheets/pdf_1/service_support_30/FSH_bro_en_5214-0482-12_v1700.pdf, accessed May 2017.

[70] International Telecommunication Union. P.531-13 (09/2016) Ionospheric propagation data and prediction methods required for the design of satellite services and systems, 2016.

[71] Basu, Santimay and MacKenzie, E. and Basu, Sunanda. Ionospheric constraints on VHF/UHF communications links during solar maximum and minimum periods. *Radio Science*, 23(3):363–378, May 1988.

[72] Sunspot Number graphics. Available online at http://www.sidc.be/silso/ssngraphics, accessed May 2017.

[73] Sreeja, V and Aquino, M. Statistics of ionospheric scintillation occurrence over European high latitudes. *Journal of Atmospheric and Solar-Terrestrial Physics*, 120:96–101, 2014.

[74] International Telecommunication Union. P.676-11 (09/2016) Attenuation by atmospheric gases, 2016.

[75] International Telecommunication Union. RECOMMENDATION ITU-R P.838-3 Specific attenuation model for rain for use in prediction methods, 2005.

[76] Wertz, James R. *Spacecraft attitude determination and control*, volume 73. Springer Science & Business Media, 2012.

[77] Aydinlioglu, Ali and Hammer, Marco. COMPASS-1 pico satellite: magnetic coils for attitude control. In *Recent Advances in Space Technologies, 2005. RAST 2005. Proceedings of 2nd International Conference on*, pages 90–93. IEEE, 2005.

[78] QB50 ADCS Interface Control Document. Available online at https://www.qb50.eu/index.php/tech-docs/category/27-up-to-date?download=133:QB50%20ADCS%20ICD%20v3.2, accessed May 2017.

[79] Hinckley, Franklin. TLE Degradations - What happens with old TLEs. 2014.

[80] Murota, Kazuaki and Hirade, Kenkichi. GMSK modulation for digital mobile radio telephony. *IEEE Transactions on communications*, 29(7):1044–1050, 1981.

[81] Rappaport, T. S. *Wireless Communications, principles and practice 2nd ed.* Prentice Hall, 2015.

[82] Norsk Radio Relæ Liga. *Norsk båndplan 2m(144-146 MHz).* Available online at `https://www.nrrl.no/images/bandplaner/BP2016-2m.pdf`, accessed May 2017.

[83] Norsk Radio Relæ Liga. *Norsk båndplan 70cm(432-438 MHz).* Available online at `https://www.nrrl.no/images/bandplaner/BP2016-70cm.pdf`, accessed May 2017.

[84] Ettus Research. *USRP Hardware Driver and USRP Manual.* Available online at `https://files.ettus.com/manual/page_general.html`, accessed May 2017.

[85] SatNOGS observation 2002. Available online at `https://network-dev.satnogs.org/observations/2002/`, accessed May 2017.

[86] SatNOGS observation 1628. Available online at `https://network-dev.satnogs.org/observations/1628/`, accessed May 2017.

[87] WXtoImg website. Available online at `http://www.wxtoimg.com/`, accessed May 2017.

[88] Stenhaug, Beathe Hagen. Antenna system for a ground station communicating with the NTNU Test Satellite (NUTS). 2011.

[89] Ploom, Indrek. Analysis of variations in orbital parameters of CubeSats. 2014.

[90] The Internationa Amateur Radio Union - Frequency Allocation for NUTS Cubesat, accessed May 2017.

[91] Owl VHF datasheet rev. B. Available online at `http://www.skagmoelectronics.com/owl/downloads/datasheet_rev_b.pdf`, accessed May 2017.

[92] TE Systems webpage. *Amateur Radio - RF AMPLIFIERS.* Available online at `http://www.tesystems.com/am-radio.htm`, accessed December 2016.

[93] Measured BER vs Sensitivity for Owl VHF. Available online at `http://skagmo.com/http_share/pcb/owl/ber.png`, accessed May 2017.

[94] Aarons, J. Global morphology of ionospheric scintillations. *Proceedings of the IEEE*, 70(4):360–378, 1982.

[95] IEEA. *GISM Techinical Manual*. Available online at `http://www.ieea.fr/help/gism-technical.pdf`, accessed December 2016.

[96] OPS-SAT website at ESA. Available online at `http://www.esa.int/Our_Activities/Operations/OPS-SAT`, accessed May 2017.

[97] Vaughan, Rodney G. Polarization diversity in mobile communications. *IEEE Transactions on Vehicular Technology*, 39(3):177–186, 1990.

[98] Giuli, Dino. Polarization diversity in radars. *Proceedings of the IEEE*, 74(2):245–269, 1986.

[99] RF Hamdesign. *PRIME FOCUS MESH DISH KIT 3 Meter DISH*. Available online at `http://www.rfhamdesign.com/downloads/rf-hamdesign-dish-kit_3m_kit_spec.pdf`, accessed May 2017.

[100] Square Kilometre Array project website. Available online at `http://skatelescope.org/`, accessed May 2017.

[101] The European VLBI Network project website. Available online at `http://www.evlbi.org/`, accessed May 2017.

[102] Akgiray, Ahmed Halid. *New technologies driving decade-bandwidth radio astronomy: quad-ridged flared horn and compound-semiconductor LNAs*. PhD thesis, California Institute of Technology, 2013.

[103] Yin, Jungang and Yang, Jian and Pantaleev, Miroslav and Helldner, Leif. The circular Eleven antenna: A new decade-bandwidth feed for reflector antennas with high aperture efficiency. *IEEE Transactions on Antennas and Propagation*, 61(8):3976–3984, 2013.

[104] Scwarzbeck Mess-Elektronik. *CTIA 0710 Dual polarized broadband horn antenna*. Available online at `http://schwarzbeck.de/Datenblatt/K0710.pdf`, accessed May 2017.

[105] Aghdam, Karim Mohammad Pour and Faraji-Dana, Reza and Rashed-Mohassel, Jalil. The sinuous antenna-A dual polarized feed for reflector-based searching systems. *AEU-International Journal of Electronics and Communications*, 59(7):392–400, 2005.

[106] Kistchinsky, Andrey. *Ultra-Wideband GaN Power Amplifiers-From Innovative Technology to Standart Products*. INTECH Open Access Publisher, 2011.

[107] Analog Devices. *HMC8205BF10 0.3 GHz to 6 GHz, 35 W, GaN Power Amplifier*. Available online at `http://www.analog.com/media/en/technical-documentation/data-sheets/HMC8205BF10.pdf`, accessed May 2017.

[108] Wolfspeed / Cree. *CMPA0060025F 25 W, 20 MHz-6000 MHz, GaN MMIC Power Amplifier*. Available online at http://www.wolfspeed.com/downloads/dl/file/id/408/product/126/cmpa0060025f.pdf, accessed May 2017.

[109] Wolfspeed / Cree. *CMPA0060002F 2 W, 20 MHz - 6000 MHz, GaN MMIC Power Amplifier*. Available online at http://www.wolfspeed.com/downloads/dl/file/id/406/product/125/cmpa0060002f.pdf, accessed May 2017.

[110] Analog Devices. *HMC659LC5 GaAs PHEMT MMIC POWER AMPLIFIER, DC - 15 GHz*. Available online at http://www.analog.com/media/en/technical-documentation/data-sheets/hmc659.pdf, accessed May 2017.

[111] Wong, Sai Wai and Zhu, Lei. Ultra-wideband power divider with good in-band splitting and isolation performances. *IEEE Microwave and Wireless Components Letters*, 18(8):518–520, 2008.

[112] Analog Devices. *HMC7149 10 WATT GaN MMIC POWER AMPLIFIER, 6 - 18 GHz*. Available online at http://www.analog.com/media/en/technical-documentation/data-sheets/HMC7149.pdf, accessed May 2017.

[113] Wolfspeed / Cree. *CMPA601C025F 25 W, 6.0 - 12.0 GHz, GaN MMIC, Power Amplifier*. Available online at http://www.wolfspeed.com/downloads/dl/file/id/410/product/128/cmpa601c025f.pdf, accessed May 2017.

[114] Low Noise Factory. *LNF-LNR1_15A 1-15 GHz Low Noise Amplifier*. Available online at http://www.lownoisefactory.com/files/5414/8978/2613/LNF-LNR1_15A.pdf, accessed May 2017.

[115] Caltech. *CIT118 Cryogenic HEMT Low Noise Amplifier*. Available online at http://radiometer.caltech.edu/datasheets/amplifiers/CIT118DataSheet.pdf, accessed May 2017.

[116] Analog Devices. *HMC753 1 GHz to 11 GHz, GaAs, HEMT, MMIC Low Noise Amplifier*. Available online at http://www.analog.com/media/en/technical-documentation/data-sheets/hmc753.pdf, accessed May 2017.

[117] Minicircuits. *PMA2-123LN+ - Low Noise, Wideband, High IP3 Monolithic Amplifier*. Available online at https://www.minicircuits.com/pdfs/PMA2-123LN+.pdf, accessed May 2017.

[118] Microsemi. *MMA043PP4 Datasheet 0.5 GHz–12 GHz GaAs pHEMT MMIC Wideband Low-Noise Amplifier*. Available online at https://www.microsemi.com/document-portal/doc_download/136883-mma043pp4-mmic-wideband-low-noise-amplifier-datasheet, accessed May 2017.

[119] Rohde & Schwarz. *R&S RTM2000 Digital Oscilloscope User Manual*. Available online at https://cdn.rohde-schwarz.com/pws/dl_downloads/dl_common_library/dl_manuals/gb_1/r/rtm_1/RTM2_UserManual_en_10.pdf, accessed May 2017.

[120] Siglent technologies CO., LTD. *SDG2000X Series Function/Arbitrary Waveform Generator*. Available online at https://mediacdn.eu/m/media/wysiwyg/siglent/Downloads/DataSheet/SDG2000X%20Datasheet-en.pdf, accessed May 2017.

[121] Rohde & Schwarz. *R&S RTB2000 Digital Oscilloscope Specification*. Available online at https://cdn.rohde-schwarz.com/pws/dl_downloads/dl_common_library/dl_brochures_and_datasheets/pdf_1/RTB2000_dat-sw_en_3607-4270-22_v0402.pdf, accessed May 2017.

[122] Ettus Research. *E310/E312*. Available online at https://kb.ettus.com/E310/E312, accessed May 2017.

[123] RFhamdesign multiband dish feed product website. Available online at http://www.rfhamdesign.com/products/dish-feeds/multiband-dish-feed/index.php, accessed May 2017.

[124] RF Hamdesign. *SPID Azimuth & Elevation antenna rotator Type: BIG-RAS/HR* . Available online at http://www.rfhamdesign.com/downloads/rf-hamdesign-dish-kit_3m_kit_spec.pdf, accessed May 2017.

[125] Hawkins, GJ and Edwards, DJ and McGeehan, JP. Tracking systems for satellite communications. In *IEE Proceedings F (Communications, Radar and Signal Processing)*, volume 135, pages 393–407. IET, 1988.

[126] Analog Devices. *HMC637ALP5E GaAs pHEMT MMIC 1 WATT POWER AMPLIFIER, DC - 6 GHz*. Available online at http://www.analog.com/media/en/technical-documentation/data-sheets/hmc637a.pdf, accessed May 2017.

[127] Pasternack SPDT Electromechanical relay. Available online at https://www.pasternack.com/sma-spdt-electromechanical-relay-switch-18-ghz-pe71s6052-p.aspx, accessed May 2017.

[128] Keysight Technologies. *Keysight PNA Series Network Analyzers*. Available online at http://literature.cdn.keysight.com/litweb/pdf/E8364-90031.pdf?id=450975, accessed May 2017.

[129] Keysight Technologies. *Keysight Technologies 85052D 3.5 mm Calibration Kit*. Available online at http://literature.cdn.keysight.com/litweb/pdf/85052-90079.pdf, accessed May 2017.

[130] ETS Lindgren. *EMC ANTENNAS DOUBLE-RIDGED WAVEGUIDE HORN Model 3117*. Available online at `http://www.ets-lindgren.com/pdf/3117.pdf`, accessed May 2017.